International Journal of Greenhouse Gas Control 65 (2017) 40–54

Contents lists available at ScienceDirect

International Journal of Greenhouse Gas Control

journal homepage: www.elsevier.com/locate/ijggc

The inherent tracer fingerprint of captured CO_2

S. Flude[a,b,*], D. Györe[b], F.M. Stuart[b], M. Zurakowska[b], A.J. Boyce[b], R.S. Haszeldine[a], R. Chalaturnyk[c], S.M.V. Gilfillan[a]

[a] School of Geosciences, The University of Edinburgh, Grant Institute, King's Buildings, James Hutton Road, EH9 3FE, UK
[b] Isotope Geosciences Unit, Scottish Universities Environmental Research Centre, Rankine Avenue, East Kilbride, G75 0QF, UK
[c] Department of Civil and Environmental Engineering, University of Alberta, Canada

ARTICLE INFO

Keywords:
Carbon capture
Geochemical tracers
Stable isotopes
Noble gases
CO_2 storage

ABSTRACT

Carbon capture and storage (CCS) is the only currently available technology that can directly reduce anthropogenic CO_2 emissions arising from fossil fuel combustion. Monitoring and verification of CO_2 stored in geological reservoirs will be a regulatory requirement and so the development of reliable monitoring techniques is essential. The isotopic and trace gas composition – the inherent fingerprint – of captured CO_2 streams is a potentially powerful, low cost geochemical technique for tracking the fate of injected gas in CCS projects; carbon and oxygen isotopes, in particular, have been used as geochemical tracers in a number of pilot CO_2 storage sites, and noble gases are known to be powerful tracers of natural CO_2 migration. However, the inherent tracer fingerprint in captured CO_2 streams has yet to be robustly investigated and documented and key questions remain, including how consistent is the fingerprint, what controls it, and will it be retained *en route* to and within the storage reservoir? Here we present the first systematic measurements of the carbon and oxygen isotopes and the trace noble gas composition of anthropogenic CO_2 captured from combustion power stations and fertiliser plants. The analysed CO_2 is derived from coal, biomass and natural gas feedstocks, using amine capture, oxyfuel and gasification processes, from six different CO_2 capture plants spanning four different countries. We find that $\delta^{13}C$ values are primarily controlled by the $\delta^{13}C$ of the feedstock while $\delta^{18}O$ values are predominantly similar to atmospheric O_2. Noble gases are of low concentration and exhibit relative element abundances different to expected reservoir baselines and air, with isotopic compositions that are similar to air or fractionated air. The use of inherent tracers for monitoring and verification was provisionally assessed by analysing CO_2 samples produced from two field storage sites after CO_2 injection. These experiments at Otway, Australia, and Aquistore, Canada, highlight the need for reliable baseline data. Noble gas data indicates noble gas stripping of the formation water and entrainment of Kr and Xe from an earlier injection experiment at Otway, and inheritance of a distinctive crustal radiogenic noble gas fingerprint at Aquistore. This fingerprint can be used to identify unplanned migration of the CO_2 to the shallow subsurface or surface.

1. Introduction

Global carbon dioxide emissions must be drastically reduced to avoid global warming (IPCC, 2013). Carbon capture and storage (CCS), increasingly combined with bio-energy (BECCS), has potential for emission mitigation (Azar et al., 2013; International Energy Agency, 2014; IPCC, 2013; Scott et al., 2012). CCS is the only currently available technology that can reduce emissions from various industrial processes, such as cement and steel manufacture and many forms of chemical synthesis. A lack of accurate and cost effective methods for monitoring the geologically stored CO_2, and unambiguously identifying the source of CO_2 in a suspected leak, remains a barrier to the roll out of CCS at commercial scales. A potential solution is to use the geochemical properties of the CO_2 itself as a geochemical tracer. Carbon ($\delta^{13}C$) and oxygen ($\delta^{18}O$) stable isotope compositions have proven to be useful tracers and monitoring tools at a number of pilot storage sites (Boreham et al., 2011; Emberley et al., 2005; Johnson et al., 2011a, 2011b; Kharaka et al., 2009, 2006; Lu et al., 2012; Martens et al., 2012; Mayer et al., 2013; Myrttinen et al., 2010; Nowak et al., 2014; Raistrick et al., 2006; Shevalier et al., 2013, 2009) and noble gases have the potential to be powerful tracers for CCS monitoring, based on their use in tracing natural CO_2 and hydrocarbon migration, tracing CO_2 during enhanced oil recovery, and ruling out a geologically deep source of fluids during a suspected leak (Gilfillan et al., 2014, 2017, 2011, 2009; Gilfillan and Haszeldine, 2011; Güleç and Hilton, 2016; Györe et al., 2017, 2015; Holland and Gilfillan, 2013; Mackintosh and Ballentine, 2012; Shelton et al., 2016).

* Corresponding author at: School of Geosciences, The University of Edinburgh, Grant Institute, King's Buildings, James Hutton Road, EH9 3FE, UK.
E-mail address: sflude@gmail.com (S. Flude).

http://dx.doi.org/10.1016/j.ijggc.2017.08.010
Received 27 January 2017; Received in revised form 14 July 2017; Accepted 17 August 2017
Available online 06 September 2017

Recent review papers collate the available information on the inherent tracer fingerprint of captured CO_2, make predictions regarding the likely fingerprint when empirical data is not available, and note the need for more direct measurements of captured CO_2 (Flude et al., 2016; Serno et al., 2017). Captured CO_2 stream generation was reviewed for conventional combustion, oxyfuel combustion, gasification (syngas production), fermentation, cement and steel manufacture, and CO_2 purification methods (chemical absorption/amine capture and physical absorption in organic solvents). It was predicted that the carbon isotope fingerprint will be controlled by the carbon-rich feedstock (e.g. fossil fuels, biomass, limestone) used in the CO_2-generating process (e.g. combustion, gasification, cement and steel manufacture, fermentation) with small isotope fractionations expected for both conversion of the feedstock to CO_2 and the CO_2 purification process (Flude et al., 2016). Oxygen isotopes were expected to be controlled by the dominant sources of oxygen in the CO_2 generation and purification processes, including water (Serno et al., 2017). Noble gases were expected to be of low concentration for most capture techniques, with the noble gases being decoupled from the CO_2 during purification; radiogenic noble gases (^{4}He and ^{40}Ar) were expected to be enriched relative to non-radiogenic noble gases in fossil fuel derived CO_2 streams, and an enrichment of Kr and Xe relative to air was expected for oxyfuel combustion CO_2 capture, introduced via cryogenically separated oxygen (Flude et al., 2016).

Here we present new carbon and oxygen isotope, and noble gas concentration and isotope data from samples collected from captured CO_2 streams from six different capture plants, including CO_2 derived from coal, biomass, and natural gas combustion with amine capture, coal oxyfuel combustion, and gasification of methane. This work aims to contribute to answering four questions: 1) What is the inherent tracer fingerprint of captured CO_2 2) What controls this fingerprint? 3) Will this fingerprint change *en route* to the storage reservoir? 4) Will this fingerprint be retained during subsurface migration in the storage reservoir?

2. Methodology

2.1. Sampling strategy

In order to determine the inherent tracer fingerprint of captured CO_2 and what controls this fingerprint, we collected CO_2 samples produced at six different capture plants, using three different feedstocks (coal, gas, and biomass) and three different capture technologies (amine capture, oxyfuel and gasification). Carbon isotopes in coal, biomass and gas feedstocks were also analysed, where available. At UKCCSRC's Pilot Scale Advanced Capture Technologies (PACT) facility (see site details below) we also collected samples of gas direct from the combustion flue (i.e. before capture) and from the exhaust of the amine absorber tank (i.e. residual gas, not absorbed during amine capture), to assess how the capture process alters the fingerprint. These samples are summarised in Table 1.

To ascertain if the fingerprint will change *en route* to the storage reservoir, we collected a sample from the CO_2 injection wellhead at the SaskPower Aquistore storage site, located in Saskatchewan, Canada, for comparison with our Boundary Dam sample (Section 2.3.2.). CO_2 from the Boundary Dam capture plant is compressed and transported to Aquistore via ~4 km of underground pipeline (Rostron et al., 2014).

In order to establish if this inherent fingerprint is retained during subsurface migration in the storage reservoir, we collected post-injection samples from the reservoir fluid sampling system in the well of the Otway 2BX-1 pilot storage project for comparison with the CO_2 injected from the Callide oxyfuel plant. A sample from the Aquistore monitoring well downhole fluid recovery system was collected for comparison with the injected Boundary Dam CO_2. Sampling site descriptions are provided in Section 2.3.

2.2. Sampling

Samples for noble gas analysis were collected using the well-established Cu-tube method (e.g. Györe et al., 2015). Gas samples were collected in 8 mm outer diameter, refrigeration grade copper tubing, connected to sampling ports (via a pressure regulator, where appropriate) with flexible high pressure hosing. An exhaust hose connected to the tube prevented turbulent back-mixing of air into the sample. The copper tube was purged with the gas stream being sampled for at least 2 min in order to flush out atmospheric contamination. The tube was then sealed with metal clamps, creating a cold-weld which is impermeable to helium. Gas samples were also collected in Tedlar gas sample bags, for stable isotope analysis, by attaching the gas bag either onto the sample port/regulator or on to the end of the copper tube exhaust pipe after the minimum flushing period. The occasions where the sampling process was modified from this standard procedure are described in the sample context descriptions below. Sample context is summarised in Table 1.

2.3. Sample source

2.3.1. Niederaussem pilot capture plant, Germany

Sample Nied#3 was collected from RWE Generation's pilot capture plant at a 1000 MW lignite-fired power plant unit at Niederaussem. This captures 90% of the CO_2 in the combustion exhaust (flue) gas and has a capture capacity of 7.2 t per day (Moser et al., 2014). The sample was collected after all washing and filtering processes, from a valve immediately before the CO_2 storage tank. A sample of lignite fuel was also collected for isotopic analysis.

2.3.2. Boundary Dam capture plant and Aquistore, Saskatchewan, Canada

Boundary Dam Power Station's 139 MW coal-fired Unit 3 is attached to the world's first commercial-scale post-combustion capture plant (Stéphenne, 2014). Samples BD1 and BD2 were collected from the Boundary Dam Capture Plant's compressor building. Here, ambient pressure CO_2 is transported from the capture plant and compressed to over 2000 psi (13.8 MPa) in stages. Both samples were collected after the CO_2 was compressed to 400 psi (2.8 MPa), dried, and accessed via a low-pressure (15–25 psi/~0.1 MPa) sample port. Sample AS_P_2 was collected from the Aquistore injection pipeline a few days after injection commenced (April 13th 2014). The pipeling transports pressurised CO_2 from the Boundary Dam Capture Plant to the Aquistore site. The sample was collected from a valve on the wellhead registering a pressure of 1608 psig (11 MPa). The pressure reduction during sampling caused dry ice to form and flow of CO_2 through the regulator slowed due to icing up; flow was maintained for long enough to collect samples but we note that sampling was under disequilibrium conditions (mixture of dry ice and gas) and so there may be some unexpected sample fractionation. Sample Tanker #1 was collected from the CO_2 used to pressurise the injection well before commencing pipeline injection into Aquistore. This CO_2 was collected from the CO_2 tanker vapour discharge valve, which registered a pressure of 230 psi (1.6 MPa) during sampling. The Tanker CO_2 was derived from the Agrium Fertiliser plant, Fort Saskatchewan, Alberta, which carries out steam reforming of methane (Agrium, 2015) A piece of the coal used as fuel at the Boundary Dam power station (BD coal) and water used to dilute the amine solution in the capture plant were also collected. In April 2014, 20 cm^3 of gas, degassed from water collected from the observation well fluid recovery system (FRS) was supplied for noble gas analysis by the University of Alberta (AQ1).

2.3.3. Ferrybridge power plant, UK

A sample of CO_2 was supplied from the CCPilot100+ pilot capture plant at the Ferrybridge Power Station, West Yorkshire, United Kingdom. The pilot capture plant operated for two years, capturing up to 90% of the CO_2 in Ferrybridge Power Station's coal-fired Unit 4 flue

Table 1
Sample name, source, feedstock and capture process context.

Captured CO_2 Samples				
Sample/type	Sample source	Feedstock	Capture process	Sample date
Nied #3	Niederaussem	Lignite (Miocene: 26-6Ma)	Amine capture	2014-09-24
BD1 & BD2	Boundary Dam	Coal (Palaeocene: 66-56 Ma)	Amine capture	2015-04-10
AS_P_2	Aquistore pipeline	Coal (Palaeocene: 66-56 Ma)	Amine capture	2015-04-21
Ferrybridge −1 & -2	Ferrybridge	Coal	Amine-capture	2013-11-29
PACT10	PACT	Biomass	Amine-Capture	2016-01-21
PACT7	PACT	Natural gas	Amine-Capture	2016-01-21
Tanker #1	Agrium Fertiliser plant	Natural gas	Gasification	2015-04-13
COSPL#1	Callide Oxyfuel Plant	Coal	Oxyfuel	2014-12-10

Fuel Samples			
Sample/type	Sample source	Feedstock	
BD Coal	Boundary Dam, Saskatchewan, Canada	Coal	2015-10-30
Nied Lignite	Niederaussem, Germany	Lignite	2014-09-24
PACT BM	PACT. Softwood forestry residue, USA	Biomass	2016-01-21
SMG	Sheffield mains gas, UK	Gas	2016-01-21

Amine Capture Process Samples			
Sample	Feedstock	Process stage	
PACT2	Biomass	Combustion flue gas	2016-01-21
PACT9	Biomass	Amine absorber outlet	2016-01-21
PACT1	Natural Gas	Combustion flue gas	2016-01-21
PACT8	Natural Gas	Combustion flue gas	2016-01-21
PACT6	Natural Gas	Amine absorber outlet	2016-01-21
BD Water		Water used to dilute amine solution	2016-01

Subsurface Samples			
Sample	Storage site	Injected CO_2	
AQ1	Aquistore	Boundary Dam (c.f. BD2/AS_P_2, ± Tanker #1)	2016-03
L-283-2	Otway 2BX-1	Callide (c.f. COSPL#1)	2014-12-5
L-284-2	Otway 2BX-1	Callide (c.f. COSPL#1)	2014-12-5

gas, and producing up to 120 t CO_2 per day via post-combustion amine capture (Fitzgerald et al., 2014). The coal being burnt during sampling was a blend of Columbian and Yorkshire coal (Mike Till, pers. comm. 2016).

2.3.4. Otway pilot injection project, Australia

The Otway Project in Victoria, Australia, is a CO_2 storage field test injection site. The Otway 2B Extension project (Otway 2BX) took place over 80 days in October − December 2014. The aim of the project was to study the effect of impurities in the CO_2 stream on water quality (days 1–62: 2BX-1) and to characterise CO_2 residual trapping (days 63–80: 2BX-2) (Serno et al., 2016). CO_2 was injected into the Paaratte Formation, employing the same reservoir and well configuration as the 2011 Otway 2 B project, which used injection and back-production from a single well to investigate CO_2 residual trapping (Paterson et al., 2013, 2011). Pure CO_2 from the Callide oxyfuel plant (Uchida et al., 2013) was injected, along with added impurities, during Otway 2BX-1 on days 11 and 36 (Haese et al., 2016). The CO_2 was co-injected with earlier-produced reservoir water that had been stored in surface tanks and mixed downhole using a gas mandrel; the experiment was designed so that all of the injected CO_2 would dissolve in the formation water on injection (Haese et al., 2016). For Otway 2BX-2, Callide CO_2 was mixed with natural CO_2 produced from the nearby Boggy Creek well (Serno et al., 2016).

Tracing injected CO_2 was not the purpose of the Otway 2BX experiments, but an impromptu opportunity arose to collect samples of CO_2 produced at the end of the Phase 1 experiment, after injection and residence in the subsurface. Subsurface CO_2 samples (L283/2 and L284/2) were collected on 5th December 2014, Day 62 of the Otway 2BX test, at the end of the initial phase (2BX-1). Reservoir water and gas samples were collected into 150 mL stainless steel cylinders at reservoir pressure (140 bar) using a downhole U-tube system (Freifeld, 2005) and degassed into 10 L gas sample bags (Serno et al., 2016). The gas from these bags was then sampled into copper tubes using the standard procedure outlined previously.

Samples of Callide CO_2 were collected in copper tubes by filling a 150 mL stainless steel Swagelok cylinder with liquid CO_2 directly from the Callide tanker, and subsequently depressurising the cylinder to flow gaseous CO_2 through the copper tube.

2.3.5. Pilot scale Advanced Capture Technologies (PACT) facility, UK

PACT is a research and development facility for carbon capture and combustion research with pilot scale combustion and solvent carbon capture plants (PACT, 2016) located in Sheffield, UK. Samples were collected while the combustion rig was burning coal or biomass in air. The first sample (PACT1) was collected from the flue pipe leading from the burner rig to the capture plant (Fig. 1) using a peristaltic pump located between the copper tube and gas bag parts of the sampling assembly. This sampling port is located after a candle filter assembly used to clean particulate material from the flue gas. Subsequent samples were collected from different sections of the PACT amine capture facility via the exhaust line of PACT's gas analysis Fourier Transform Infra

Red spectroscopy (FTIR) instrument, during line purging (Fig. 1). A piece of hosing connected the FTIR exhaust to the sampling tube assembly. An exhaust hose prevented turbulent back mixing of gas into the sample tube, and allowed venting of the flowing gas outside of the instrumentation hut. During sampling, the FTIR line, exhaust and sample assembly were purged with the desired gas for a total 4 min. After two minutes, a Tedlar bag was attached to the exhaust line of the sampling assembly to collect samples for stable isotope analysis (approximate sampling time of 30 s), followed by clamping of the copper tube to collect samples for noble gas analysis. An extra sample of natural gas combustion flue gas, equivalent to PACT1, was collected via the FTIR (PACT8) because the PACT1 Tedlar bag failed to retain the gas. This sample was collected at the end of natural gas combustion operation, while biomass was being fed into the boiler and it is thus possible that this sample has been contaminated by biomass flue gas. During sample collection, the absorber column was at a temperature of 35–48 °C and the desorber column was running at 91–99 °C. No sampling ports were available at the PACT facility to collect the mains gas burnt in the rig, so a sample was collected by connecting a piece of hosing to a gas stove top (Sheffield Mains Gas − SMG). A piece of the biomass used as fuel was also sampled.

2.4. Analytical methods

2.4.1. Stable isotopes

Stable isotope composition of captured CO_2, feedstocks, and water were analysed in the stable isotope laboratories at the University of Calgary, Canada, and at the Scottish Universities Environment Research Centre (SUERC), East Kilbride, UK.

For the PACT samples, gas compositional analysis was carried out at the Applied Geochemistry Laboratory at the University of Calgary. The analysis was undertaken using a Bruker 450 gas chromatograph (GC), which was calibrated immediately prior to analysis, and drift monitored every ten samples, using a certified formation gas standard. Reproducibility of the samples are typically ~5.0%.

At the University of Calgary Isotope Science Laboratory, CO_2 samples were purified on a glass extraction line to produce pure aliquots of CO_2. Water samples were equilibrated with CO_2 for $\delta^{18}O_{H2O}$ measurements. C- and O- isotopes were then analysed by Dual Inlet Isotope Ratio Mass Spectrometry (DI-IRMS) using a DeltaV+ stable isotope ratio mass spectrometer. Internal laboratory reference materials, that are periodically calibrated to international reference materials, were run at the beginning and end of each sample set and were used to normalize the data relative to V-PDB and V-SMOW and correct for any instrument drift. Precision and reproducibility are better than ± 0.1‰ for both $\delta^{13}C$ and $\delta^{18}O$.

At SUERC, solid samples (coal and lignite) were converted into CO_2 gas for stable isotope analysis. 2–5 milligrams of coal were added to a quartz glass tube, along with pre-roasted wire-form copper oxide. The tube was sealed and roasted at 850 °C for 1.5 h, followed by 12 h of cooling. The copper oxide reacted with the carbon in the coal to form CO_2, which can be analysed to give the C-isotope composition of the bulk coal. All CO_2 samples (oxidised from coal and original gas samples) were purified on a glass, vacuum extraction line to produce pure CO_2. Samples were then isotopically analysed using a VG Isotech Sira II DI-IRMS using standard techniques. Based on repeat analyses of internal and international standards during the running of these samples, precision and reproducibility are typically around ± 0.2‰ for both $\delta^{13}C$ and $\delta^{18}O$.

For oxygen isotope water analyses, 200 µL of the water sample was decanted into a 10 mL exetainer® using an adjustable pipette with disposable pipette tips. The exetainers® were then placed in the autosampler tray of a Thermo Scientific Delta V mass spectrometer, set at 25 °C. Each sample was then over-gassed with a 1% CO_2-in-He mixture for 5 min and left to equilibrate for a further 24 h before analysis. Oxygen isotopic data were then produced using the method established by Nelson (2000). Reproducibility of the data, based on within-run repeat analyses of at least three standard waters, was around ± 0.2‰ for $\delta^{18}O$. All results are presented in standard delta notation, relative to V-PDB (for $\delta^{13}C$, and in the supplementary information for $\delta^{18}O$) and V-SMOW (for $\delta\ ^{18}O$).

2.4.2. Noble gases

Copper tubes were connected to an all-metal ultra-high vacuum system and prepared for noble gas analysis at SUERC as described previously (Györe et al., 2015). Where necessary, three aliquots of the gas were then trapped into glass ampules for stable isotope analysis, using liquid nitrogen and sealing the ampule with a blowtorch after pumping away the other volatile gases. The remaining gas from the copper tube was cleaned using a titanium sublimation pump and getters, to remove all substances other than the noble gases, which were then stored in a stainless steel cylinder. The concentration and isotopic composition of noble gases was determined on an MAP 215-50 noble gas mass spectrometer. Analytical procedures for He, Ne, Ar, Kr and Xe isotopic analysis are described in previous work (re et al., 2017, 2015; re et al., 2017, 2015) and reproducibility of noble gas concentrations and isotope ratios is typically better than 0.5% for He, Ne and Ar, and better than 5% for Kr and Xe.

3. Results

3.1. Stable isotopes

Full stable isotope data, and gas concentration data when undertaken, are provided in Supplementary Data Tables 1–3 and are summarised in Tables 2–4. Gas concentration results from PACT (Supplementary Table S1) indicate that the samples collected from the FTIR exhaust contain a significant proportion of atmospheric contamination. However, given the low concentration of CO_2 in the atmosphere, this CO_2 contamination is small can be easily corrected for using a simple

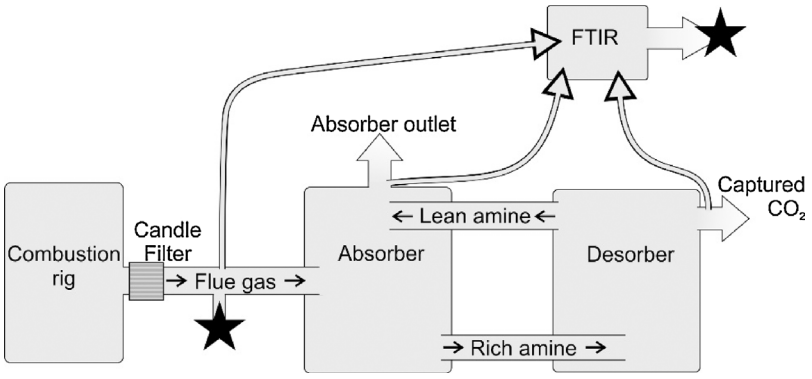

Fig. 1. Schematic of the PACT facility with sampling locations indicated by stars.

two end-member mixing model:

$$\delta^{13}C_{CO_2-measured} = \frac{(\delta^{13}C_{CO_2-sample} \times [CO_{2-sample}]) + (\delta^{13}C_{CO_2-air} \times [CO_{2-air}])}{[CO_{2-measured}]} \quad (1)$$

where square brackets indicate fractions of the component where [$CO_{2-measured}$] = 1. The fractions of CO_2 from sample and air were estimated by comparing the expected CO_2 concentrations, where available (~9% CO_2 for gas rig combustion flue, 99% CO_2 for captured CO_2, based on usual operation of the PACT capture plant) with the measured values. This indicates that between 70 and 80% of the collected sample is air contamination. The PACT stable isotope results presented in Tables 2 and 3 are corrected values.

The measured CO_2 concentrations for the absorber outlet were higher than the expected values. Assuming an expected flue gas composition of ~9 vol% CO_2, and a 90% capture efficiency, the absorber outlet CO_2 concentration would be expected to be ~0.9 vol%. The measured values were between 1 and 2.4%. Air has a CO_2 concentration of ~0.04 vol%, lower than that expected in the absorber outlet samples. The higher than expected CO_2 concentrations cannot thus be explained by air contamination and we infer that the amine capture process was not running at full efficiency during our sampling period.

Stable isotope results of captured CO_2 are shown in Table 2. $\delta^{13}C$ ranges from −38.05 to −23.1‰ and $\delta^{18}O$ ranges from +17.6 to +40.1‰.

Stable isotope results from different parts of the CO_2 generation and capture process (fuel, flue gases, absorber exhaust gases, solvent) are compared to the captured CO_2 results in Table 3. Solid fuels (biomass, lignite, coal) range in $\delta^{13}C$ from −26.7 to −23.5‰ while natural gas is −40.6‰. Flue gases range from $\delta^{13}C$ = −27.3 to −25.3 and $\delta^{18}O$ = +24.0 to +29.0‰.

Stable isotope data from the post-injection subsurface CO_2 samples collected from the Otway 2BX-1 experiment are compared to the injected CO_2 in Table 4. $\delta^{13}C$ is ~ −24‰ and $\delta^{18}O$ is ~ +35‰.

3.2. Noble gases

Noble gas data are presented in Tables 5 and 6. Noble gases were not analysed in the air-contaminated PACT samples.

Noble gas results are reported as concentrations (cm^3 per cm^3 at standard temperature and pressure: STP − 273.15 K and 1 atmosphere) and isotope ratios in Tables 5 and 6. Helium isotope ratios are expressed as R/R_A, where R is the $^3He/^4He$ value of the sample and R_A is the $^3He/^4He$ value of air (1.39×10^{-6} −Mamyrin et al., 1970).Data are conventionally represented graphically as isotope ratio variation diagrams, as concentrations normalised to air and as noble gas concentrations in the sample normalised to ^{36}Ar and air i.e.:

$$\frac{(Sample\ noble\ gas/Sample^{36}Ar)}{(Air\ noble\ gas/Air^{36}Ar)} \quad (2)$$

Noble gas concentrations in the captured CO_2 are typically two to three orders of magnitude lower than in air, while isotope ratios are similar to air. The natural gas fuel sample (SMG) has a helium content higher than air by two orders of magnitude but the other noble gases are of low concentration. Noble gas concentrations and isotope ratios other than $^3He/^4He$ in the analysed flue gas are similar to air. The post-injection subsurface gases have variable noble gas concentrations and isotopic compositions. The AQ1 sample is notably similar to air.

4. Discussion

4.1. Composition and controls on the tracer fingerprint of captured CO_2

4.1.1. Carbon isotopes

Fig. 2 shows the C-isotope composition of the analysed captured CO_2 samples, along with C-isotope data for fuel feedstocks, where appropriate. Flude et al. (2016) predicted that the C-isotope composition of CO_2 captured from combustion power plants would be mostly controlled by the fuel feedstock with possible fractionation during both combustion and amine capture. They predicted $\delta^{13}C_{Combustion\_CO2}$ values of −31 to −21‰ for coal, less than −21‰ for natural gas, and −24 to −30‰ for C3 biomass combustion (Flude et al., 2016), with subsequent amine capture potentially imparting an extra fractionation of between −20 and +2.5‰. CO_2 captured from gasification plants was predicted to show a possible small negative fractionation, producing captured CO_2 with $\delta^{13}C$ < -20‰. All of the coal and gas combustion-derived captured CO_2 falls within the range of values expected for combustion CO_2, based on worldwide ranges of fuel $\delta^{13}C$. CO_2 captured from biomass combustion falls outside of the values expected for combustion, but within the range of values expected due to fractionation during amine capture.

Specific feedstock C-isotope data are available to compare with amine captured CO_2 from combustion of biomass (c.f. PACT10), lignite (c.f. Nied#3), coal (c.f. BD1) and natural gas (c.f. PACT7). Fig. 3 shows the difference in $\delta^{13}C$ (Δ) between captured CO_2 and the fuel, and for intermediate stages of the combustion and capture process, where available, ranked in terms of their hydrocarbon maturity. $\Delta_{Captured\text{-}Fuel}$ range from −5.0‰ (biomass) to +2.6‰ (natural gas) with an apparent increase in Δ value with increasing hydrocarbon maturity. Coal shows the least fractionation between fuel and captured CO_2. CO_2 in the pre-capture combustion flue gas was also analysed for biomass (PACT2) and natural gas combustion (PACT8). Δ values were calculated for Flue gas-Fuel and for Captured CO_2-Flue gas to investigate the influence of these different processes (combustion and amine capture) on the C-isotope value. In both cases $\Delta_{Flue\text{-}fuel}$ is positive (+1.4‰ for biomass, +13.3‰ for gas), opposite to the expected −1.3‰ fractionation during combustion (Flude et al., 2016; Widory, 2006). $\Delta_{Captured\text{-}Flue}$ is negative in both cases (-6.4‰ for biomass, −10.7‰ for gas). This is consistent with the predicted fractionation of between −20 and +2.5‰ (Flude et al., 2016). The greatest fractionations observed during combustion and capture are for the gas-combustion sample. As

Table 2
Stable isotope composition of captured CO_2. Data with uncertainties (1σ) are averages of multiple analyses. Data without uncertainties represent single data points. Full data are provided in Supplementary Table 3.

Sample	Process	Fuel	$\delta^{13}C$ V-PDB ‰	$\delta^{18}O$ V-SMOW ‰
BD2	Amine capture	Coal	−23.4 ± 1.5	+17.8 ± 1.9
AS_P_2	Amine capture	Coal	−23.4 ± 0.3	+17.6 ± 0.8
Nied#3	Amine Capture	Lignite	−27.4 ± 1.3	+18.7 ± 1.8
Ferrybridge-1	Amine Capture	Coal	−25.3 ± 0.4	+24.1 ± 0.1
PACT10	Amine Capture	Biomass	−31.7	+25.3
PACT7	Amine Capture	Gas	−38.1	+26.3
Tanker #1	Gasification	Gas	−24.1 ± 0.6	+18.9 ± 1.1
COSPL #1	Oxyfuel	Coal	−26.7 ± 0.4	+27.3 ± 0.1

Table 3
Stable isotope data from the fuel to capture process. AO = Absorber Outlet and refers to the gas released from the amine absorber column exhaust. Data with uncertainties (1σ) are averages of multiple analyses. Data without uncertainties represent single data points. Full data are provided in Supplementary Table 3.

Sample	Fuel	Point	δ^{13}C V-PDB	δ^{18}O V-SMOW
BD Coal	Coal	Fuel	−23.4 ± 0.0	
BD2	Coal	Captured	−23.4 ± 1.5	+17.8 ± 0.8
BD Water		Solvent		−27.8 ± 0.3
Nied Lignite	Lignite	Fuel	−24.0 ± 0.1	
Nied #3	Lignite	Captured	−27.4 ± 1.3	+18.7 ± 1.8
PACT BM	Biomass	Fuel	−26.7	
PACT2	Biomass	Flue	−25.3	+24.0
PACT9	Biomass	AO	−23.6	+24.3
PACT10	Biomass	Captured	−31.7	+25.3
SMG	Gas	Fuel	−40.6	
PACT8	Gas	Flue	−27.3	+25.6
PACT6	Gas	AO	−36.0	+26.4
PACT7	Gas	Captured	−38.0	+26.3

Table 4
Stable isotope composition of injected and subsurface fluids from Otway. Data are averages of multiple analyses and uncertainties are 1σ. Full data are provided in Supplementary Table 3.

Sample	Stage	δ^{13}C V-PDB	δ^{18}O V-SMOW
COSPL #1	Injected	−26.7 ± 0.4	+27.3 ± 0.1
L-283-2	Lift gas	−24.4 ± 1.1	+35.1 ± 0.4
L-284-2	Lift gas	−23.7 ± 0.2	+35.2 ± 0.4

previously outlined, the flue sample (PACT8) may be contaminated with biomass flue gas and this value should be interpreted with caution.

The effect of amine capture on the $\delta^{13}C_{CO2}$ was investigated by comparing δ^{13}C values for flue gas, absorber outlet and captured CO_2 samples derived from biomass (samples PACT2, 9 and 10). Absorption of CO_2 by amine solutions involves formation of bicarbonate and carbamate species in the solution (Lee et al., 2013). Carbamate-CO_2 enrichment factors of +11‰ have been reported (Usdowski and Hoefs, 1988) while bicarbonate − CO_2 enrichment factors for fresh water at 35 to 45 °C range from 6.9 to 5.9‰ (calculated from Clark and Fritz, 1997). Assuming that these enrichment factors are appropriate for amine capture and that CO_2 desorption is more efficient than CO_2 absorption, it should be possible to determine the efficiency of the CO_2 capture process by comparing the δ^{13}C values of the flue, absorber

Table 5
Noble gas concentration data. Concentrations are volume fractions and given in cm^3 (STP)/cm^3. Standard temperature and pressure is as reported in Ozima and Podosek (2002). Air composition is after Ozima and Podosek (2002) and references therein, and air saturated water (ASW) is calculated after Kipfer et al. (2002). Uncertainties are one standard deviation.

Sample name.	^{4}He	^{3}He	^{20}Ne	^{40}Ar	^{36}Ar	^{132}Xe	^{84}Kr
AIR	5.24E-06 ± 5.00E-08	7.33E-12 ± 5.17E-14	1.65E-05 ± 3.62E-08	9.34E-03 ± 1.00E-05	3.13E-05 ± 3.35E-08	2.34E-08 ± 2.69E-10	6.50E-07 ± 5.70E-09
ASW 10 °C	4.60E-08	6.50E-14	1.80E-07	3.80E-04	1.30E-06	3.60E-09	5.20E-08
ASW 60 °C	4.00E-08	5.70E-14	1.30E-07	1.70E-04	5.70E-07	1.20E-09	1.80E-08
Captured CO_2							
BD #1	2.29E-09 ± 1.11E-10	3.04E-15 ± 6.91E-16	7.50E-09 ± 3.18E-10	8.67E-06 ± 3.21E-07	2.90E-08 ± 1.08E-09	2.82E-11 ± 1.48E-12	5.28E-10 ± 2.19E-11
AS-P-2	8.41E-09 ± 4.08E-10	1.99E-14 ± 3.54E-15	1.14E-08 ± 4.82E-10	7.93E-06 ± 2.93E-07	2.72E-08 ± 1.03E-09	4.40E-11 ± 2.30E-12	5.26E-10 ± 2.19E-11
Nied#3	3.08E-08 ± 1.49E-09	1.52E-14 ± 4.21E-15	2.64E-09 ± 5.72E-11	4.33E-06 ± 8.22E-08	1.45E-08 ± 3.33E-10	3.32E-11 ± 1.74E-12	3.59E-10 ± 1.49E-11
Ferrybridge #2	3.76E-08 ± 1.82E-09	6.53E-14 ± 4.39E-15	4.24E-08 ± 1.80E-09	1.71E-05 ± 6.32E-07	5.94E-08 ± 2.21E-09	3.64E-11 ± 1.91E-12	9.19E-10 ± 3.82E-11
Tanker#1	3.01E-07 ± 1.46E-08	3.55E-13 ± 1.97E-14	2.39E-07 ± 1.01E-08	7.83E-05 ± 2.90E-06	2.75E-07 ± 1.02E-08	1.21E-09 ± 6.36E-11	3.77E-09 ± 1.57E-10
COSPL #1 2/2	3.64E-07 ± 1.77E-08	4.20E-13 ± 8.29E-14	4.27E-07 ± 1.81E-08	1.37E-04 ± 5.08E-06	4.79E-07 ± 1.78E-08	1.91E-09 ± 9.98E-11	6.34E-09 ± 2.64E-10
Fuel							
SMG	1.28E-04 ± 6.23E-06	1.09E-11 ± 4.23E-13	3.34E-08 ± 1.42E-09	6.31E-05 ± 2.33E-06	1.42E-07 ± 5.30E-09	4.04E-10 ± 2.12E-11	5.23E-09 ± 2.17E-10
Flue Gas							
PACT-01	6.35E-06 ± 3.08E-07	3.87E-12 ± 2.61E-13	6.48E-06 ± 3.21E-07	3.55E-03 ± 1.31E-04	1.19E-05 ± 4.38E-07	2.43E-07 ± 1.25E-08	4.07E-07 ± 1.70E-08
Subsurface gases							
AQ1	7.48E-05 ± 2.78E-06	4.59E-11 ± 4.00E-12	3.00E-06 ± 6.50E-08	1.55E-03 ± 5.73E-05	5.36E-06 ± 2.00E-07	3.19E-09 ± 1.67E-10	8.65E-08 ± 3.60E-09
L283/2	1.73E-07 ± 8.37E-09	2.05E-13 ± 1.26E-14	2.22E-07 ± 9.46E-09	2.31E-04 ± 8.56E-06	7.77E-07 ± 2.89E-08	1.10E-07 ± 5.75E-09	2.48E-07 ± 1.03E-08

Table 6
Noble gas isotope data. Air composition is after Ozima and Podosek (2002) and references therein and Lee et al. (2006), and air saturated water (ASW) is calculated after Kipfer et al. (2002). Uncertainties are one standard deviation.

Sample name	$^{3}He/^{4}He$ R/R_A	$^{20}Ne/^{22}Ne$	$^{21}Ne/^{22}Ne$	$^{40}Ar/^{36}Ar$	$^{38}Ar/^{36}Ar$	$^{84}Kr/^{132}Xe$	$^{4}He/^{20}Ne$
AIR	1.000 ± 0.0093	9.805 ± 0.080	0.029 ± 0.0003	298.56 ± 0.31	0.1885 ± 0.0003	27.78 ± 0.40	3.18E-01 ± 3.12E-03
ASW 10 °C	0.980	9.805	0.029	298.56	0.1885	14.44	2.56E-01 ± 0.00E+00
ASW 60 °C	0.990	9.805	0.029	298.56	0.1885	15.00	3.08E-01 ± 0.00E+00
Captured CO_2							
BD #1	0.949 ± 0.2108	9.75 ± 0.116	0.029 ± 0.001	298.76 ± 1.35	0.1842 ± 0.0038	18.68 ± 1.25	3.05E-01 ± 1.97E-02
AS-P-2	1.696 ± 0.2895	10.008 ± 0.083	0.030 ± 0.000	290.94 ± 1.97	0.1834 ± 0.0110	11.97 ± 0.80	7.41E-01 ± 4.77E-02
Nied#3	0.352 ± 0.0963	9.638 ± 0.261	0.028 ± 0.001	298.21 ± 3.84	0.0116 ± 0.0058	10.80 ± 0.72	1.17E+01 ± 6.20E-01
Ferrybridge #2	1.241 ± 0.0566	10.263 ± 0.123	0.030 ± 0.001	287.42 ± 0.90	0.1831 ± 0.0032	25.26 ± 1.69	8.87E-01 ± 5.72E-02
Tanker#1	0.842 ± 0.0214	10.108 ± 0.120	0.030 ± 0.001	284.26 ± 0.82	0.1843 ± 0.0025	3.11 ± 0.21	1.26E+00 ± 8.14E-02
COSPL #1 2/2	0.824 ± 0.1574	10.150 ± 0.121	0.029 ± 0.001	286.52 ± 0.88	0.1853 ± 0.0031	3.33 ± 0.22	8.54E-01 ± 5.51E-02
Fuel							
SMG	0.061 ± 0.0038	9.570 ± 0.079	0.031 ± 0.001	443.09 ± 1.82	0.1854 ± 0.0045	12.95 ± 0.87	3.84E+03 ± 2.48E+02
Flue Gas							
PACT-01	0.436 ± 0.0364	9.567 ± 0.083	0.029 ± 0.001	299.38 ± 0.88	0.1864 ± 0.0028	1.67 ± 0.11	9.80E-01 ± 6.79E-02
Subsurface gases							
AQ1	0.438 ± 0.0417	9.714 ± 0.082	0.029 ± 0.001	288.64 ± 1.49	0.1906 ± 0.0076	27.16 ± 1.82	2.49E+01 ± 1.07E+00
L283/2	0.849 ± 0.0311	9.814 ± 0.117	0.029 ± 0.001	297.64 ± 1.18	0.1873 ± 0.0038	2.26 ± 0.15	7.76E-01 ± 5.01E-02

outlet, and captured CO_2. In this case, the $\delta^{13}C$ of the flue gas CO_2 would be the initial reacting CO_2, the absorber outlet reflects the residual CO_2 remaining after absorption, and the captured CO_2 represents the amine dissolved inorganic carbon (DIC) (assuming that significant fractionation does not take place during desorption). A Rayleigh fractionation model was created to try and reproduce the absorber outlet and captured CO_2 $\delta^{13}C$ values, using Eq. (3) (Clark and Fritz, 1997).

$$\delta - \delta_0 \approx \varepsilon \times \ln(f) \quad (3)$$

Where δ is the $\delta^{13}C$ of the residual reactant (in this case the absorber outlet gas), δ_0 is the initial $\delta^{13}C$ of the reactant gas (in this case the flue gas), ε is the enrichment factor, and f is the fraction of reactant remaining. It was not possible to reproduce the residual reactant (absorber outlet) and dissolved carbon (captured CO_2 as a proxy) $\delta^{13}C$ values using the expected enrichment factors, which are both positive. It is possible that DIC-CO_2 enrichment factors are different for amine solutions and fresh water, and that enrichment factors for amine capture can be estimated by iterative calculation of Rayleigh fractionation models with different enrichment factors until there is convergence between measured and modelled absorber outlet and captured CO_2 (DIC) values. Results of this modelling are shown in Fig. 4, which suggests a DIC-CO_2 enrichment factor during absorption of −7‰ and that only ~20% of the CO_2 was being captured at the time of sampling. This may indicate that the PACT absorber column was not operating at full capacity during sampling, an interpretation backed up by the discrepancy between expected (0.9%) and measured (up to 2.4%) CO_2 concentrations in the absorber outlet samples (Section 3.1).

4.1.2. Oxygen isotopes

Fig. 5 shows the O-isotope composition of captured CO_2, compared to natural sources of oxygen. Combustion of C-rich fuels should produce CO_2 with $\delta^{18}O$ similar to that of atmospheric oxygen, with a possible fractionation of up to −21‰ for combustion of low ignition temperature fuel and/or combustion in an oxygen-rich environment (Serno et al., 2017). Boundary Dam and Niederaussem captured CO_2 are consistent with this hypothesis, but three amine-captured and one oxyfuel combustion CO_2 samples have $\delta^{18}O$ higher than that of atmospheric oxygen (Ferrybridge, PACT, Callide). $\delta^{18}O$ values of flue gases collected at PACT are also higher than that of atmospheric oxygen, suggesting either that oxygen isotope behaviour during combustion is not straightforward, or that passing of flue gas through a candle filter causes isotope fractionation.

Sample COSPL is CO_2 captured from the Callide Oxyfuel Plant, Australia, which uses a cryogenic air separation unit to supply high purity O_2 for combustion, and a cryogenic CO_2 separation unit to purify the end produced CO_2 (Uchida et al., 2013). It is possible that large-scale cryogenic separation causes O-isotope fractionation, with the heavier isotopes preferentially partitioning into the cryogenically trapped phase, resulting in $\delta^{18}O$ enrichment of the purified O_2 and CO_2.

The $\delta^{18}O$ of CO_2 produced by gasification processes is expected to be dominated by that of the water (steam) used during steam reforming and the shift reaction (Flude et al., 2016; Serno et al., 2017). The $\delta^{18}O$ of Tanker#1 is particularly surprising as this value (+19‰) is significantly higher than the global range of meteoric water and is similar to atmospheric O_2, as would be expected for a gasification plant that used partial oxidation instead of steam reforming for the gasification process (Serno et al., 2017). Alternatively it is possible that the fertilizer plant uses an isotopically unusual source of water to generate steam, or that significant O-isotope fractionation occurs during steam reforming, with ^{16}O being preferentially retained in the water phase and ^{18}O preferentially combining with natural gas derived carbon to form CO_2.

(Serno et al., 2017) noted that the O-isotope composition of amine-captured CO_2 should be influenced by any water in the CO_2 generation system, and thus it is difficult to predict due to the wide range of $\delta^{18}O$ of meteoric waters and a lack of known amine solution-CO_2 enrichment or fractionation factors. At the current time, enrichment factors between the water in amine solutions and captured CO_2 have not been published, perhaps due to difficulties in measuring $\delta^{18}O_{aminesolution}$. We analysed $\delta^{18}O$ in a sample of demineralised water from Boundary Dam's water treatment plant, which is used to dilute amine solution for the CO_2 capture process. This water has a notably light O-isotope composition ($\delta^{18}O$ = −28‰) and the difference between the water and CO_2 captured from Boundary Dam is ~ +46‰. This degree of enrichment can only be produced between fresh water and CO_2 at temperatures of ~ 0 °C (calculated via Clark and Fritz, 1997), much lower than the temperatures involved during amine capture (35–50 °C and 90–110 °C for the absorber and desorber, respectively). This suggests that either the amine solution-CO_2 enrichment factors are much greater than for fresh water-CO_2 systems, or that isotopic equilibrium is not reached during the capture process. Alternatively, contrary to predictions, the O-isotope composition of flue gas CO_2 dominates the O-isotope budget of the system. In hindsight, this result is not surprising as amine absorber columns are designed to maximise gas-water contact areas (Fitzgerald et al., 2014) and thus the gas to water ratio will be large,

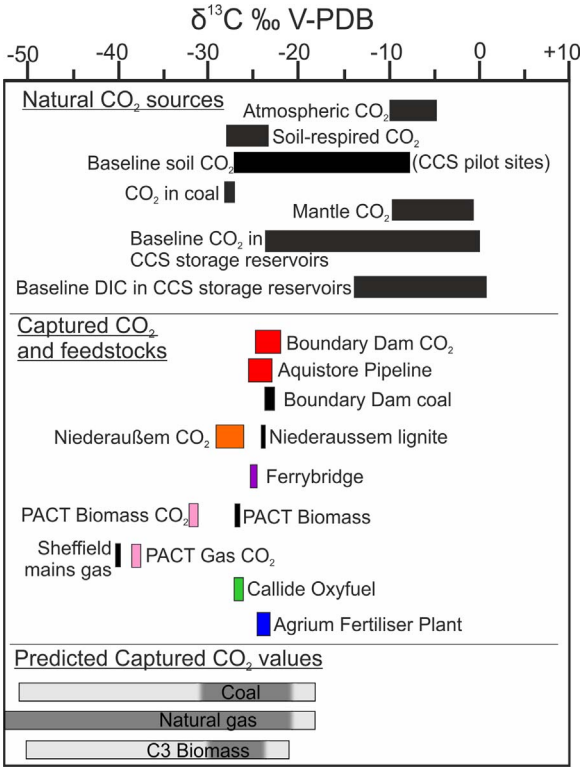

Fig. 2. C-isotope composition of captured CO_2 and feedstock compared to natural CO_2 sources. Baseline and predicted values from Flude et al. (2016). Dark grey predicted values represent the anticipated C-isotope composition of CO_2 produced during combustion. Light grey areas represent additional fractionation that may take place during amine capture. Boundary Dam CO_2 = Sample BD2. Aquistore Pipeline = Sample AS_P_2. Niederaussem CO_2 = Sample Nied#3. Ferrbyridge = Sample Ferrybridge-1. PACT Biomass CO_2 = Sample PACT10. PACT Gas CO_2 = Sample PACT7. Callide Oxyfuel = -Sample COSPL#1. Agrium Fertiliser Plant = Sample Tanker#1. (For interpretation of the references to color in this figure legend, the reader is referred to the web version of this article.).

resulting in the isotopic composition of the gas dominating the system. This hypothesis is consistent with the very small difference in $\delta^{18}O$ values observed between flue gas CO_2 and captured CO_2 for the PACT samples (Fig. 5).

4.1.3. Noble gases

Fig. 6 shows normalised concentrations of noble gases in the captured CO_2, while Fig. 7 shows selected noble gas isotope ratios.

Flude et al. (2016) made predictions regarding the noble gas content of captured CO_2. Conventional fuel combustion is expected to

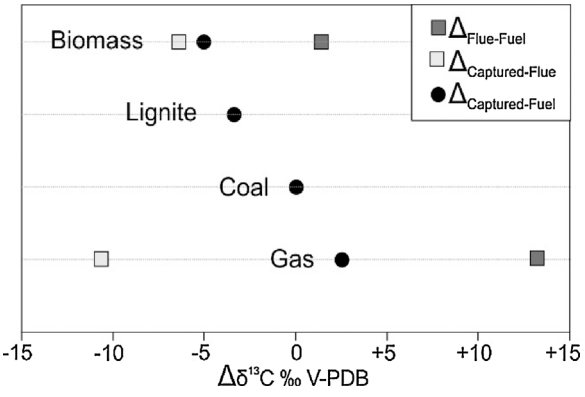

Fig. 3. Difference (Δ) between average fuel, flue gas, and captured CO_2 $\delta^{13}C$ values for fuel combustion with CO_2 amine capture.

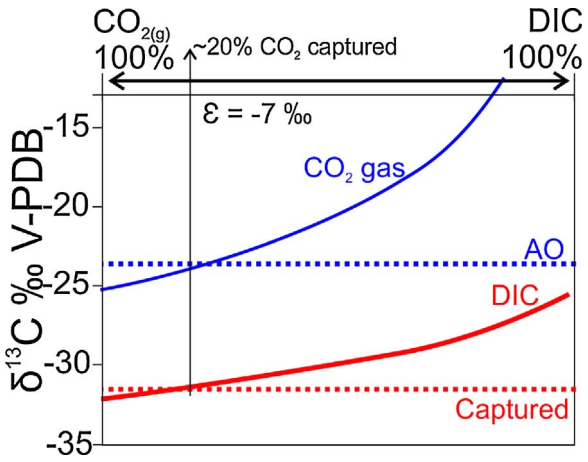

Fig. 4. Rayleigh fractionation model to calculate an estimation of the DIC-CO_2 enrichment factor for amine capture of CO_2. Dotted lines are measured values. Solid lines are calculated Rayleigh fractionation curves for a starting flue gas CO_2 with $\delta^{13}C$ of −25.3‰ dissolving into amine solution with an iteratively calculated DIC-CO_2 enrichment factor of −7‰. (For interpretation of the references to color in this figure legend, the reader is referred to the web version of this article.).

incorporate air-like noble gases into the flue gas, while oxyfuel combustion will introduce noble gases via the source of O_2. Use of fossil fuel feedstocks is expected to produce a relative enrichment of He, and possibly Ar, due to the accumulation of radiogenic ^4He and ^{40}Ar in the fossil fuel. Use of coal as a feedstock may give an enrichment in heavy noble gases, which have a high adsorption affinity for fine-grained organic material and coals (Flude et al., 2016; Podosek et al., 1981).

Noble gases in amine-captured CO_2 were predicted to be of especially low concentration (much lower than air saturated water −ASW), with a possible small relative enrichment in heavy over light noble gases (upward slope from left to right on Fig. 6A and B), due to mass-dependent differences in noble gas solubility (Flude et al., 2016). Our new data mostly agree with this prediction; Boundary Dam (BD2), Ferrybridge (Ferrybridge-1) and Niederaussem (Nied#3) CO_2 streams all have noble gas concentrations up to two orders of magnitude lower

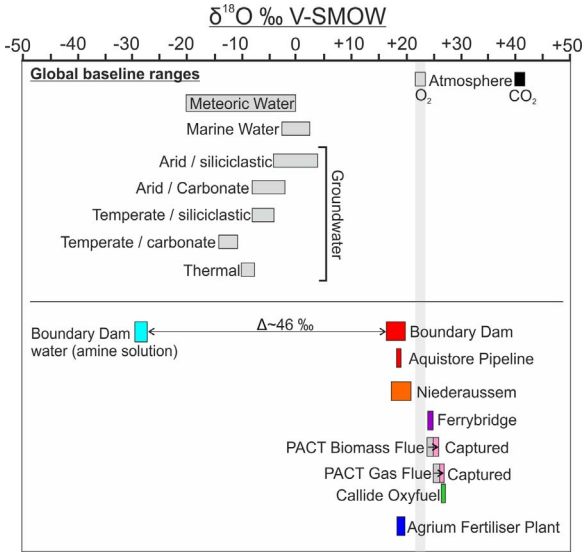

Fig. 5. Oxygen-isotope values for the captured CO_2 along with combustion flue gases where available, and amine solution values. Baseline ranges from (Ciais et al., 1997; Clark and Fritz, 1997; Drimmie et al., 1991; Ettayfi et al., 2012; Kroopnick and Craig, 1972; Newell et al., 2014; Nisi et al., 2013; Serno et al., 2017). PACT Biomass Flue = Sample PACT2. PACT Gas Flue = Sample PACT8. See Fig. 2 caption for other sample designations. (For interpretation of the references to color in this figure legend, the reader is referred to the web version of this article.).

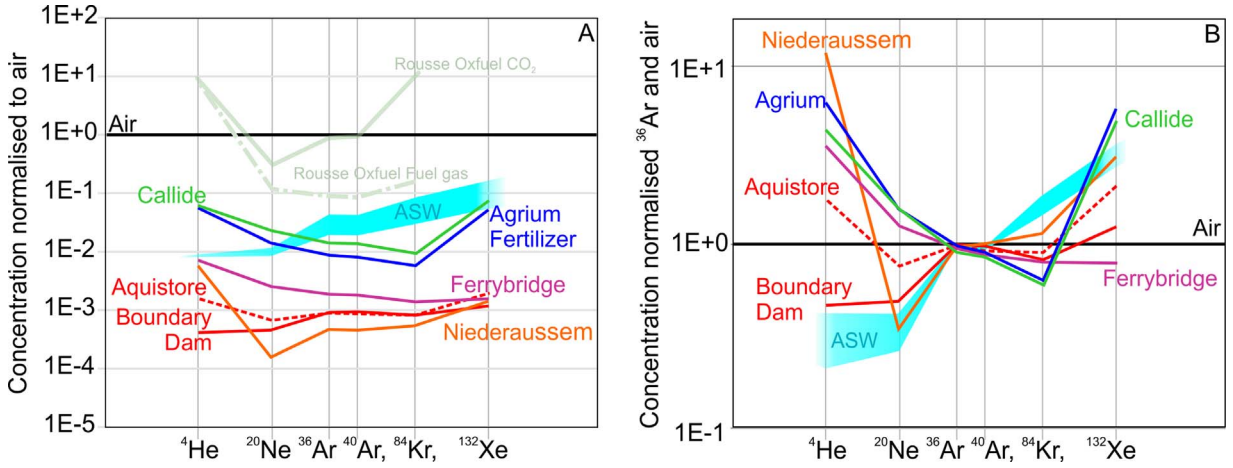

Fig. 6. Noble gas concentrations in capture CO_2 normalised to concentrations in air (A) and normalised to ^{36}Ar and air (B). Rousse data from Garcia et al. (2012). The range of air saturated water (ASW) noble gas concentrations for water equilibrated with air at between 10 and 60 °C (calculated according to Kipfer et al., 2002) is also shown. Ferrybridge = Sample Ferrybridge-2. All other samples are as described in Fig. 2. (For interpretation of the references to color in this figure legend, the reader is referred to the web version of this article.).

than ASW (Fig. 6A). The relative concentrations of noble gases in the sample from Niederaussem also fit this prediction well, with an elevated ^4He content and an increase in abundance relative to air from Ne to Xe (Fig. 6A and B).

Noble gas concentrations in oxyfuel produced CO_2 were expected to be high – possibly of higher concentration than in air, especially for Kr and Xe which may be concentrated in cryogenically separated oxygen (Flude et al., 2016). This was corroborated by noble gas data for oxyfuel CO_2 produced at Laq, France, which showed enrichment of all noble gases above the natural gas fuel, and krypton concentrations an order of magnitude higher than found in air (Garcia et al., 2012) (Fig. 6). Our oxyfuel sample (COSPL) has the highest noble gas concentrations of all our captured CO_2 samples, but concentrations remain one to two orders of magnitude below air concentrations (Fig. 6A). Helium concentrations were expected to be dependent on the radiogenic He content of the fuel, while the remaining noble gases were expected to show a relative enrichment in heavier noble gases (an upward slope from Ne to Xe on Fig. 6A and B). However, an overall decrease in slope from Ne to Kr is observed, with a relative enrichment in Xe. The difference between our measured oxyfuel noble gas values, and those of the Laq oxyfuel may represent differences in post-capture purification of the CO_2, or differences in oxygen purification techniques used to generate O_2 for the oxyfuel combustion process resulting in different trace noble gas concentrations in the purified O_2.

Noble gases in CO_2 produced by gasification (steam reforming) were expected to be of low concentrations, similar to that of ASW, and with relative elemental abundances similar to ASW. The measured concentrations are within an order of magnitude of ASW, but the relative elemental abundances show the opposite trend to ASW, with enrichment of light and depletion of heavy noble gases, other than Xe, which is also enriched. The feedstock for the Tanker#1 CO_2 was natural gas. Enrichment of Xe is often observed for natural gases (Torgersen and Kennedy, 1999) and so this observed Xe enrichment likely derives from the organic content of the feedstock.

Noble gas isotope ratios were expected to be air like but with enrichment of radiogenic ^4He and possibly ^{40}Ar in CO_2 derived from fossil fuels (Flude et al., 2016). Fig. 7 plots He, Ar and Ne isotope ratios relative to air and air saturated water. Enrichments in $^{40}Ar/^{36}Ar$ over air, due to addition of radiogenic ^{40}Ar were not observed. This is likely due to the low K-content of fossil fuels combined with the long half life of ^{40}K (1.25×10^9 years – McDougall and Harrison, 1999) leading to a slow build up of ^{40}Ar in the fuel (c.f. coal age of 6.6×10^7 years), combined with the relatively high concentration of Ar in the atmosphere (0.934% – Ozima, M. and Podosek, 2002) and the high level of atmospheric input in most CO_2 production processes. The majority of samples Exhibit $^{40}Ar/^{36}Ar$ ratios significantly below the atmospheric value (298.56 – Lee et al., 2006) indicating that isotopic mass fractionation takes place at some point in the CO_2 generation and purification process.

Helium isotope ratios (presented as R/R_A – Fig. 7) in samples Nied#3, COSPL and Tanker#1 show a small enrichment in ^4He ($R/R_A < 1$), as expected. Samples Ferrybridge-1 and AS-P-2 both have $^3He/^4He$ ratios greater than the atmospheric value. Ferrybridge-1 plots close to the mass fractionation line, calculated using Graham's law (Holland and Gilfillan, 2013). Ne isotope data (Fig. 7) also indicate that most samples have noble gas isotope ratios consistent with fractionated air.

Unfortunately, it was not possible to analyse noble gases on a full suite of samples including fuel, flue gas, and end product captured CO_2, to assess how different stages of the CO_2 production and capture process control the noble gas fingerprint of the captured CO_2 stream. Samples SMG and PACT1 represent natural gas fuel and the flue gas derived from combustion of this gas in air; the associated sample of captured CO_2 (PACT7) was, unfortunately, too contaminated with air to provide meaningful noble gas data, having been sampled via the FTIR exhaust (see Sections 2.3.5 and 3.1). However, comparison of the noble gas concentrations and ratios between SMG and PACT1 may provide some constraints (Fig. 8).

Sample SMG has low concentrations (less than ASW) for all noble gases other than He, which shows an enrichment in ^4He, as would be expected for a gas that has resided in the geological subsurface. Argon and helium isotopes also show radiogenic isotope enrichment ($^{40}Ar/^{36}Ar > 298.56$; $^3He/^4He << 1$ R/R_A – see Fig. 8 and Table 6). The flue gas sample has a higher $^3He/^4He$ ratio, but this is still less than the atmospheric $^3He/^4He$ ratio, suggesting that the radiogenic ^4He signature has been retained, albeit diluted. The flue gas $^{40}Ar/^{36}Ar$ value is atmospheric, indicating that the argon fingerprint of the natural gas has been diluted beyond recognition due to mixing with air during combustion. A simple two component mixing model between SMG and air (Fig. 8) was calculated to assess whether the He and Ar isotopes in sample PACT1 could be explained by mixing between SMG and air during combustion. The flue gas plots on the mixing line at ~3% SMG and 97% air. However, the noble gas concentrations cannot be reproduced using this mixing model.

A mixing model invoking 60% SMG and 40% air best fits the concentrations of Ne and Ar, but this model over-estimates He and underestimates Kr and Xe. A potential source for the excess Kr and Xe is the candle filter between the combustion rig and the flue gas sampling port. Kr and Xe have high adsorption affinities (Podosek et al., 1981) and it is possible that Kr and Xe released from fuel in previous combustion

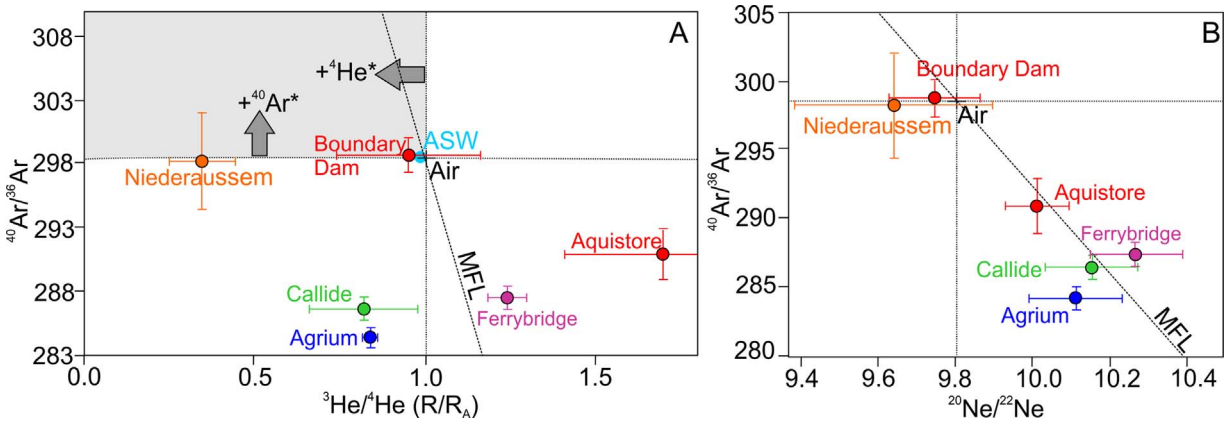

Fig. 7. Isotope ratio variation diagrams for He, Ne and Ar in the captured CO_2 streams. MFL = mass fractionation line. R/R_A represents the $^3He/^4He$ value of the sample normalised to that of the atmosphere. The grey box shows the field that noble gases in fossil-fuel derived CO_2 streams were expected to plot in (Flude et al., 2016). Samples are as described in Fig. 6. (For interpretation of the references to color in this figure legend, the reader is referred to the web version of this article.).

experiments were trapped in the candle filter via adsorption onto the high surface area porous interior, or adsorption onto the fine grained particles trapped by the filter. These adsorbed noble gases would then be released into the gas stream when encountering a hotter or lower Kr and Xe concentration gas.

4.2. Fingerprint retention during transport

Transport of captured CO_2 from the capture plant to the storage site is most likely to be via pipeline or tanker. In either case, the CO_2 will be pressurised and transported as either a liquid or supercritical fluid. Sample BD1 was collected from the Boundary Dam capture plant compressor building, immediately before the final stages of compression for pipeline transport. Transport of CO_2 from the compressor building to the Aquistore injection site is via ~5 km long underground pipeline (Whittaker and Worth, 2011) maintained at ~2200 psi (15 MPa – SaskPower, pers. comm.). Sample AS_P_2 was collected 11 days later from the Aquistore injection wellhead. The coal used as fuel at Boundary Dam is sourced locally from large open cast coal mines, and so variation in fuel type or quality is not expected to influence the CO_2 fingerprint.

Recent work has identified differences in solubility of noble gases between low and high density CO_2 (Warr et al., 2015), and so open-system fluctuations in CO_2 density may result in significant elemental fractionation of the noble gases. As noted in Section 2.3.2, dry ice formed during sampling of AS_P_2 and the sample was thus not collected under equilibrium conditions meaning that any fractionation effects will likely be enhanced. Carbon and oxygen isotopes (Figs. 2 and 4) show negligible variation between the two samples, suggesting that the C and O isotope fingerprint of the captured CO_2 will be preserved during transport.

Figs. 6 and 7 compare the noble gas content of the samples. Concentrations of Ar and Kr show good agreement but He, Ne and Xe are all higher in concentration in sample AS_P_2. Noble gas isotopes also show differences between the two samples with AS_P_2 having lower $^{40}Ar/^{36}Ar$, and higher $^3He/^4He$ and $^{20}Ne/^{22}Ne$. AS_P_2 lies on the mass fractionation line on both Ar and Ne isotope variation diagrams (Fig. 7), suggesting that kinetic isotope fractionation of noble gases may take place during pipeline transport and/or CO_2 stream phase changes as the noble gases diffuse between the different phases. However, it is likely that these modifications to the noble gas fingerprint occurred during the sampling procedure, rather than transport. The pressurised pipeline is a relatively closed and simple system compared to the sampling port and equipment, where the CO_2 experienced a pressure drop from 1608 psig (11 MPa) to atmospheric pressure and a phase change from supercritical phase to a mixture of dry ice and gas. Nevertheless, the possibility of elemental and isotopic fractionation should be taken into account, especially when sampling injected CO_2 from pressurised

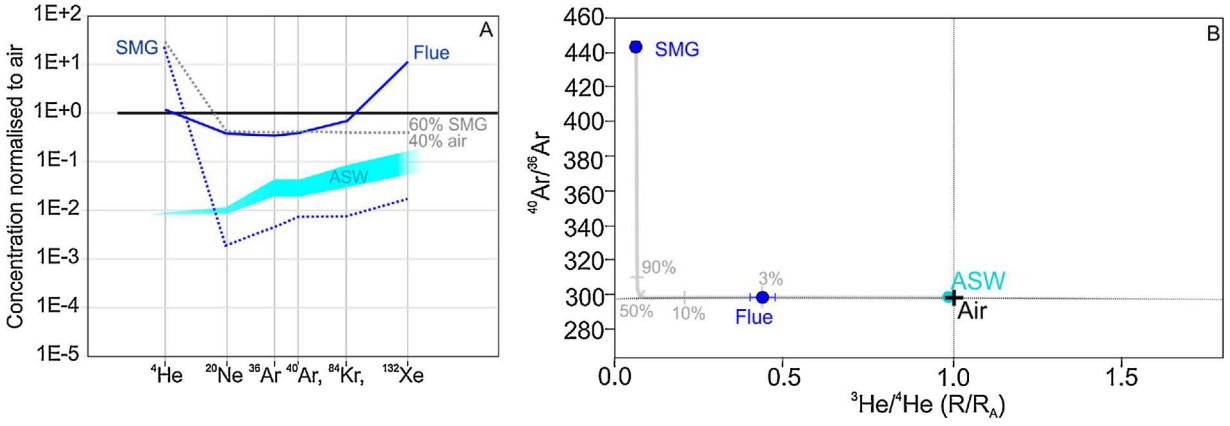

Fig. 8. Noble gas concentrations (A) and isotope ratios (B) for the Sheffield mains gas (SMG) burnt in the gas rig at PACT to generate flue gas sample PACT 1 (Flue). The dotted grey line in the left hand panel represents a two end member mass-balance mixing model between 60% SMG and 40% air that provides the best fit to sample PACT1. The grey line in the right hand panel is a model mixing line between noble gases in sample SMG and air, with tick marks representing the proportion of SMG. The He and Ar isotopes of sample PACT 1 are consistent with mixing between 3% mains gas and 97% air. (For interpretation of the references to color in this figure legend, the reader is referred to the web version of this article.).

sources, such as injection wellheads.

4.3. Is the inherent fingerprint retained during subsurface migration in the storage reservoir?

Three of the captured CO_2 streams that we sampled have been injected into geological storage pilot sites. Pressurisation of the Aquistore pipeline (Saskatchewan, Canada) was undertaken using 37 m^3 of Tanker#1 CO_2 (Agrium Fertilizer Plant), followed by injection of pipeline transported Boundary Dam CO_2. At the Otway pilot injection site, Australia, Callide CO_2 (COSPL) was injected as part of the Otway Phase 2B extension experiment. Both pilot storage sites are equipped with downhole fluid recovery systems to facilitate sampling of geological fluids and the CO_2 in the storage reservoir.

4.3.1. Otway 2BX

Samples L283/2 and L284/2 were collected from the Paaratte Formation, via the U-tube system (Freifeld, 2005), 26 days after the second injection of Callide CO_2 (COSPL) as part of the Otway 2BX-1 experiment. Hence, these potentially provide a measure of how the inherent fingerprint of the Callide CO_2 sample evolves on injection and subsequent production from a subsurface storage reservoir.

Carbon isotope values are slightly higher (by 2.4–3.0‰) in the reservoir samples (-24.4 to −23.7‰) than the injected Callide CO_2 (-26.7‰). Subsurface processes that can cause a shift in $\delta^{13}C_{CO2}$ are mixing with a source of CO_2 that has a different isotopic signature, and isotopic fractionation during partial dissolution or exsolution. Fractionation during dissolution of the CO_2 is expected to be negligible as the experiment was designed to promote full dissolution of the CO_2 upon injection (see Section 2.3.4). C-isotope fractionation may have occurred during collection of the gas sample if incomplete degassing of the pressurised fluid occurred and a significant proportion of DIC remained in the fluid phase. Paterson et al. (2011) concluded that all Paaratte Formation water DIC was bicarbonate. Enrichment factors between bicarbonate and CO_2 gas ($\varepsilon_{HCO2\text{-}CO2}$) will be positive at temperatures less than ~100 °C, meaning that CO_2 will be isotopically lighter, and thus have a lower $\delta^{13}C$, than co-existing bicarbonate. Our reservoir samples are isotopically heavier (higher $\delta^{13}C$) than the presumed DIC and so the difference in isotope values cannot be explained by incomplete degassing during sample collection. Baseline $\delta^{13}C$ data have not been published for the Otway 2 experiment series, but naturally occurring CO_2 from a range of formations in the Otway basin have $\delta^{13}C$ between −16 and 0‰ (Watson et al., 2004). It is thus most likely that the observe difference in $\delta^{13}C$ between the injected and produced CO_2 is due to mixing in the reservoir with a naturally occurring, heavier CO_2 source.

$\delta^{18}O$ values in the reservoir samples are higher than in the Callide sample (Fig. 9). Oxygen readily exchanges between CO_2 and water and the resulting isotopic shifts can be used to calculate freephase CO_2 pore space saturation (Johnson et al., 2011a; Serno et al., 2016). $\delta^{18}O$ values for Paaratte formation waters during Otway 2BX1 phase 1 showed little variation over the duration of the experiment (−6.2 to −5.7‰, Serno et al., 2016). Serno et al. (2016) calculated a $\delta^{18}O_{CO2\text{-}H2O}$ enrichment factor for the Paaratte formation of ε = 36.84‰. Assuming isotopic equilibrium is established between the formation water and the injected CO_2, the maximum expected $\delta^{18}O_{CO2}$ value is that of the water plus the calculated enrichment factor. This gives a maximum expected $\delta^{18}O_{CO2}$ of 31‰, but the measured $\delta^{18}O_{CO2}$ is ~35‰. This 4‰ difference may reflect undocumented natural sample variability, isotopic fractionation during diffusion of the CO_2 through the formation waters, as hypothesised and observed for C-isotopes (Freundt et al., 2013; Mayer et al., 2015; Myrttinen et al., 2010), or a separate source of oxygen. The second CO_2 injection of the Otway 2BX-1 experiment included added impurities of 9 ppm NO_2, 67 ppm SO_2 and 6150 ppm O_2 (Haese et al., 2016). The O-isotope composition of these added oxygen sources, and the extent to which they will isotopically exchange with the water and CO_2 is unknown.

Noble gas data for the injected CO_2 (COSPL) and the post-injection reservoir gas (L283/2) are compared in Fig. 10. The noble gas fingerprint of injected CO_2 is expected to mix with the reservoir noble gases with an anticipated increase in radiogenic isotopes (^4He, ^{21}Ne and ^{40}Ar). Baseline noble gas data are unfortunately not available. Post injection, the reservoir CO_2 has lower He and Ne and higher Ar, Kr and Xe than the injected CO_2, which is unexpected. The xenon concentration (0.1 ppm) is notably high and an order of magnitude greater than in air. The source of this excess Kr and Xe is likely residual gas from the 2011 Otway 2B experiment, where Kr and Xe were added as tracers to measure CO_2 residual saturation.

During the 2B experiment, the noble gases were measured via gas chromatography (GC) mass spectrometry, with Kr and Xe detection limits of ~1 ppm (Paterson et al., 2011). Our measured Kr and Xe concentrations in sample L283/2 are very high for geological fluids and compared to air, but remain below the GC detection limits, meaning that post-experiment alteration to the reservoir noble gas baseline by the 2B experiment would not be detectable without noble gas mass spectrometry analysis. Some of the impurities added in the second part of the Otway 2BX-1 (Haese et al., 2016) experiment may also contribute additional Kr and Xe. For example, oxygen and nitrogen are often cryogenically separated from air and may preferentially concentrate the heavy noble gases.

The lack of expected ^4He enrichment in the subsurface gases may be due to gas stripping of the subsurface fluids during the Otway 2B injection experiment. The Paaratte formation is 1075–1472 m deep and so is expected to have accumulated radiogenic ^4He. Noble gas solubility in water and brine increases with increasing mass, and it is likely that the lighter noble gases (He and Ne) preferentially partitioned into the newly injected gas phase during the 2011 Otway 2 B experiment and were effectively stripped from the reservoir during back-production of the injected CO_2. This would result in a He and Ne depleted (and Kr and Xe enriched) baseline for the 2BX experiments and emphasises the need for accurate baseline determination when using noble gases as tracers, especially when working in geological formations that have been disturbed by human activity.

4.3.2. Aquistore

The Aquistore observation well is situated 150 m northeast of the injection well (Rostron et al., 2014) and is fitted with a downhole fluid recovery system (FRS) (Worth et al., 2014). A sample of CO_2 and methane, degassed from fluid collected at the FRS in April 2016, one year after injection commenced at Aquistore, was provided by the University of Alberta for noble gas analyses.

Noble gases in the injected CO_2 (Tanker #1/Agrium, AS_P_2/Aquistore Pipeline and BD1/Boundary Dam) are compared to the subsurface sample (AQ1) in Fig. 10. The Aquistore storage reservoir is within sandstones of the Cambro-Ordovician Deadwood and Winnipeg formations (Jensen and Rostron, 2014), which directly overlie the Precambrian basement (Worth et al., 2014). It was not possible to collect a baseline sample for noble gas analysis before CO_2 injection took place and we have thus used published noble gas data from Canadian Shield brines (Greene et al., 2008) as an estimate of the Aquistore noble gas baseline data.

In Fig. 10, the relative proportions of Ne through to Xe in AQ1 are comparable to air (i.e. the slope of the AQ1 line is parallel to that of air, despite lower absolute concentrations) and concentrations of most noble gases are higher than the injected CO_2, estimated reservoir baseline, or ASW. Ne isotope ratios and $^{84}Kr/^{132}Xe$ are atmospheric, but $^{40}Ar/^{36}Ar$ is sub-atmospheric, suggesting isotope fractionation of atmospheric Ar has taken place. These observations suggest that this sample has been heavily contaminated with atmospheric noble gases. This air contamination may have been introduced during the sampling procedure, if the copper tube was not sufficiently vented prior to sealing, or post sampling, if the copper tube was not fully sealed.

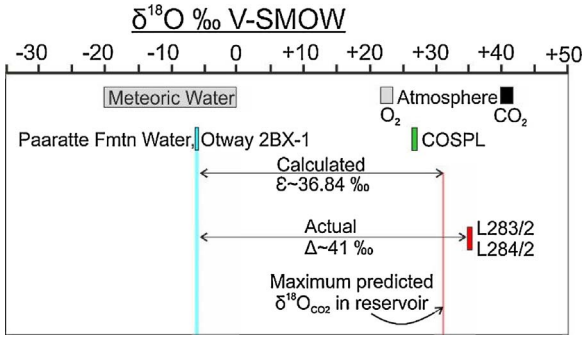

Fig. 9. Oxygen isotope data for injected and post-injection reservoir CO_2 in the Otway 2BX-1 experiment. Paaratte Formation water values from (Serno et al., 2016). COSPL = Callide CO_2 (injected). L283/2 and L284/2 are reservoir samples collected via u-tube. (For interpretation of the references to color in this figure legend, the reader is referred to the web version of this article.).

Alternatively, atmospheric noble gases may have been introduced to the sample in the fluid recovery system, which uses nitrogen (which is often derived from air), as a lift gas.

The noble gas concentrations in AQ1 can be approximately reproduced by a hypothetical model involving mixing of 80% injected CO_2 (the relative proportions of BD1 and Tanker#1 make negligible difference to the model results), 15% air and 5% baseline noble gases, assuming that the baseline is similar to the Canadian Shield Brines measured by Greene et al. (2008). We note that the true baseline may be very different and that this is not a unique model solution.

While the air contamination in this sample makes it difficult to use noble gases to assess subsurface mixing and migration, we note that sample AQ1 has a low $^3He/^4He$ ratio (0.44 R/R_A) and a high ^4He concentration (75 ppm, an order of magnitude higher than the concentration in air). This is consistent with our prediction that injected CO_2 will inherit the noble gas fingerprint of the reservoir. If this CO_2 were to subsequently leak to the surface, we would expect the elevated ^4He and below air $^3He/^4He$ ratio to be retained during this vertical migration and facilitate identification of the leaking gas as having a geologically deep source, as has been observed for natural leakage at Teapot Dome, Wyoming (Mackintosh and Ballentine, 2012), and St John's, Arizona/New Mexico (Gilfillan et al., 2011).

5. Conclusions and implications

We find that the $\delta^{13}C$ values in captured CO_2 are mostly controlled by the feedstock composition, as previously predicted (Flude et al., 2016). However, we also find that a small fractionation between fuel and CO_2 (−5 to +2.6‰) may occur. This appears to be distinct from the previously observed fractionation of −1.3‰ during combustion

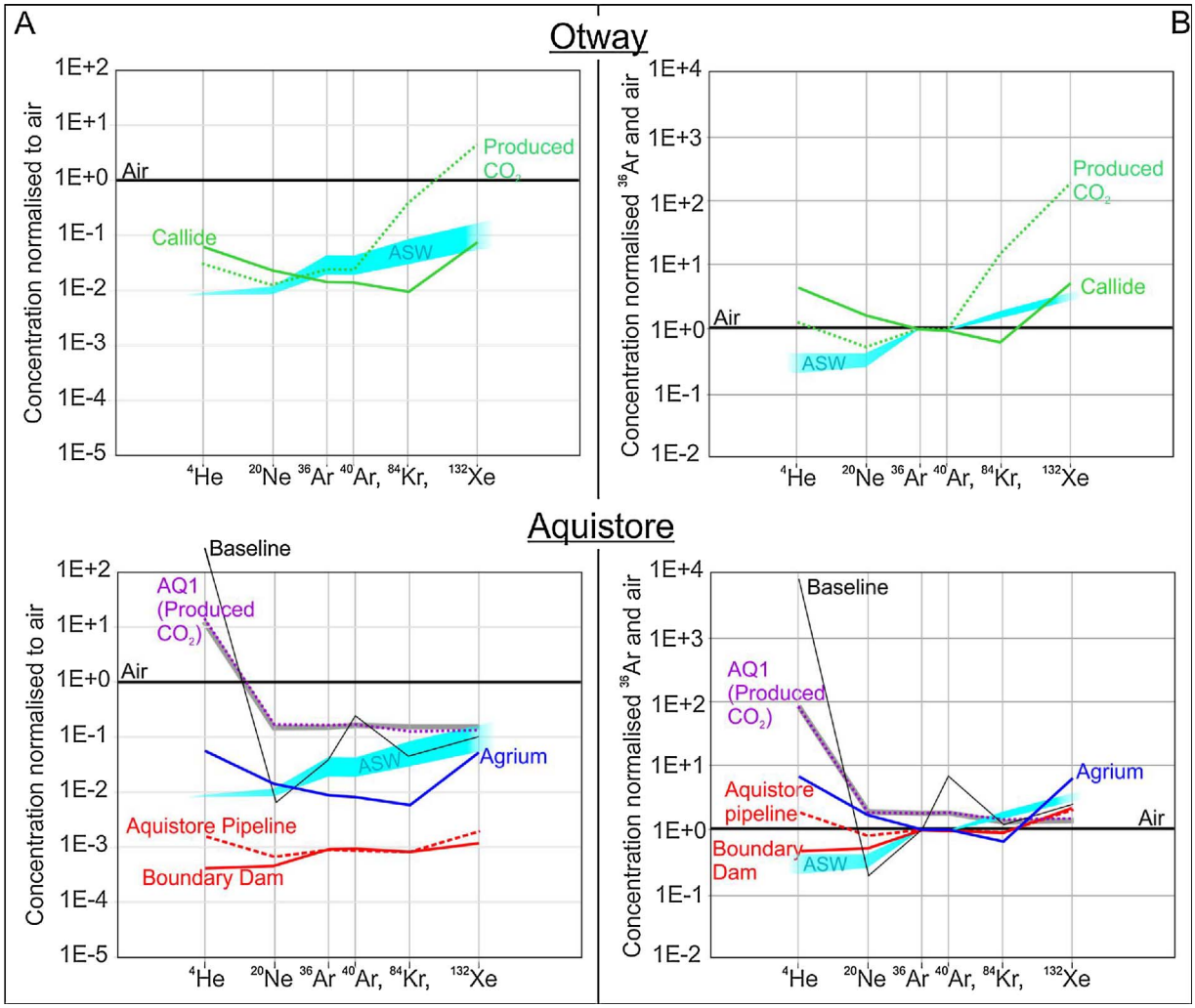

Fig. 10. Comparison of noble gas concentrations in injected and post-injection reservoir CO_2 for Otway 2BX-1 and Aquistore. Grey line represents a mixing model between 80% injected CO_2 (proportions of Tanker#1 and BD1 make little difference), 5% baseline and 15% air. (For interpretation of the references to color in this figure legend, the reader is referred to the web version of this article.).

(Widory, 2006). The majority of the CO_2 samples exhibit $\delta^{18}O$ similar to atmospheric O_2, although captured CO_2 samples from biomass and gas feedstocks at one location in the UK are significantly higher.

The $\delta^{18}O$ of combustion derived CO_2 in flue gas was expected to be similar to or lower than the $\delta^{18}O$ of atmospheric O_2. with amine capture being predicted to control $\delta^{18}O$ of captured CO_2 via O-isotope exchange with the water in the amine solution (Serno et al., 2017). However we find that the difference in $\delta^{18}O$ between the water used to dilute the Boundary Dam amine solution, and the Boundary Dam captured CO_2 is larger than can be explained by equilibrium O-isotope exchange between water and CO_2. Hence, it appears that amine capture exerts little influence on the O-isotope composition of captured CO_2, and that combustion flue gas CO_2 may have $\delta^{18}O$ higher than that of atmospheric O_2, contrary to the expected fractionation (Serno et al., 2017). The reason for this is unknown but may relate to fractionation during filtering/cleaning of the flue gas. CO_2 derived from a fertiliser plant via steam reforming has a $\delta^{18}O$ surprisingly similar to that of atmospheric O_2, suggesting that the O-isotope composition of CO_2 produced by gasification is not, as predicted (Serno et al., 2017), controlled by the water used during steam reforming.

Our measured noble gas concentrations in captured CO_2 are generally as expected from previous work (Flude et al., 2016), apart from an oxyfuel sample which exhibited lower concentrations than expected. Relative noble gas elemental abundances are variable and often show an opposite trend to that of ASW. Expected enrichments in radiogenic noble gases (^4He and ^{40}Ar) for fossil fuel derived CO_2 (Flude et al., 2016) are not always observed due to dilution with atmospheric noble gases during the CO_2 generation and capture process. In the case of combustion, the majority of this dilution takes place during fuel ignition. Noble gas isotope ratios indicate that isotopic fractionation takes place during the CO_2 generation and capture process, resulting in isotope ratios similar to fractionated air. Phase changes associated with CO_2 transport and sampling may induce noble gas elemental and isotopic fractionation, due to different noble gas solubilities between high (liquid or supercritical) and low (gaseous) density CO_2.

Samples from two CCS injection sites were collected to assess how effectively the inherent CO_2 fingerprint is retained after injection into the storage formation, but full interpretation of the data was hampered by a lack of reliable baseline data (Otway 2BX) and air contamination of the sample (Aquistore). Nevertheless, data from Otway 2BX indicate that $\delta^{13}C$ values of the CO_2 changed slightly once injected due to mixing with pre-existing CO_2. Furthermore, noble gas data from the post-injection Otway storage reservoir identify noble gas stripping of the Paaratte formation and contamination with Kr and Xe related to an earlier injection experiment. Finally He data from Aquistore illustrate that injected CO_2 will inherit distinctive crustal radiogenic noble gas fingerprints from the subsurface once injected into a geological storage reservoir.

Inherent tracers thus have the potential to be valuable geochemical monitoring tools for tracking the fate and migration of CO_2 injected into the subsurface for storage but further research from test injection sites is needed to resolve how inherent tracers can be most effectively used to monitor commercial scale CO_2 storage. We conclude that the majority of captured CO_2 sources will have carbon and oxygen isotope compositions that fall within a relatively restricted range ($\delta^{13}C$: −40 to −20‰; $\delta^{18}O$: +15 to +30‰), despite generation from a range of feedstocks and processes. These ranges show some overlap with, but are at least partially distinct from expected natural baselines and so can be expected to act as useful geochemical tracers in the majority of cases. Noble gas elemental and isotopic compositions will be distinct from reservoir baseline values, and so may prove to be valuable inherent tracers, but more work is needed to assess the sensitivity of this technique due to the low noble gas concentrations in captured CO_2. We also recommend further work is carried out into the baseline noble gas conditions of CO_2 storage reservoirs in depleted oil and gas reservoirs where hydrocarbon production may have stripped out initial reservoir noble gases. In such situations, the distinctive radiogenic signature associated with deep crustal fluids, and which is a reliable tracer of CO_2 origin for naturally occurring CO_2 seeps, may no longer be present. Finally, we note that carbon and oxygen isotopes and noble gases may also act as tracers for industrial and capture processes. Whilst the goal of our data analysis was to understand what controls the geochemical and isotopic fingerprint of captured CO_2 streams to improve prediction of this fingerprint, in doing so we illustrate that these geochemical tracers may have potential for assessing process efficiency in industrial applications relevant to CO_2 capture.

Acknowledgements

The following people and organisations are thanked for their assistance and cooperation with supply and collection of CO_2 samples: Mike Till, SSE; Darcy Holderness, SaskPower; Kyle Worth, PTRC; Gonzalo Zambrano Narvaez and Kais Ben Andallah, The University of Alberta; Peter Moser, Sandra Schmidt and George Wiechers, RWE Niederaussem; Kris Milkowski, Muhammad Akram, Martin Murphy and János Szuhánszki, PACT; Jay Black, Hong Phuc Vu and the field operating team under the supervision of Rajindar Singh at the CO2CRC Otway site. Mike Nightingale and Steve Taylor are thanked for carrying out the gas concentration and stable isotope analyses at the University of Calgary. Terry Donnelly, Alison McDonald and Rory McKavney are thanked for their contribution to stable isotope analyses at SUERC. This work was supported by EPSRC grant #EP/K036033/1.

Appendix A. Supplementary data

Supplementary data associated with this article can be found, in the online version, at http://dx.doi.org/10.1016/j.ijggc.2017.08.010.

References

Agrium, 2015. Fort Saskatchewan Nitrogen Operations: Brochure.

Azar, C., Johansson, D.J.A., Mattsson, N., 2013. Meeting global temperature targets—the role of bioenergy with carbon capture and storage. Environ. Res. Lett. 8, 034004. http://dx.doi.org/10.1088/1748-9326/8/3/034004.

Boreham, C., Underschultz, J., Stalker, L., Kirste, D., Freifeld, B., Jenkins, C., Ennis-King, J., 2011. Monitoring of CO_2 storage in a depleted natural gas reservoir: gas geochemistry from the CO2CRC Otway Project, Australia. Int. J. Greenhouse Gas Control 5, 1039–1054. http://dx.doi.org/10.1016/j.ijggc.2011.03.011.

Ciais, P., Denning, A.S., Tans, P.P., Berry, J.A., Randall, D.A., Collatz, G.J., Sellers, P.J., White, J.W.C., Trolier, M., Meijer, H.A.J., Francey, R.J., Monfray, P., Heimann, M., 1997. A three-dimensional synthesis study of $\delta^{18}O$ in atmospheric CO_2: 1. Surface fluxes. J. Geophys. Res. 102, 5857. http://dx.doi.org/10.1029/96JD02360.

Clark, I.D., Fritz, P., 1997. Environmental Isotopes in Hydrogeology.

Drimmie, R.J., Aravena, R., Wassenaar, L.I., Fritz, P., James Hendry, M., Hut, G., 1991. Radiocarbon and stable isotopes in water and dissolved constituents, Milk River aquifer, Alberta, Canada. Appl. Geochem. 6, 381–392. http://dx.doi.org/10.1016/0883-2927(91)90038-Q.

Emberley, S., Hutcheon, I., Shevalier, M., Durocher, K., Mayer, B., Gunter, W.D., Perkins, E.H., 2005. Monitoring of fluid–rock interaction and CO_2 storage through produced fluid sampling at the Weyburn CO_2-injection enhanced oil recovery site, Saskatchewan, Canada. Appl. Geochem. 20, 1131–1157. http://dx.doi.org/10.1016/j.apgeochem.2005.02.007.

Ettayfi, N., Bouchaou, L., Michelot, J.L., Tagma, T., Warner, N., Boutaleb, S., Massault, M., Lgourna, Z., Vengosh, A., 2012. Geochemical and isotopic (oxygen, hydrogen, carbon, strontium) constraints for the origin, salinity, and residence time of groundwater from a carbonate aquifer in the Western Anti-Atlas Mountains, Morocco. J. Hydrol. 438-439, 97–111. http://dx.doi.org/10.1016/j.jhydrol.2012.03.003.

Fitzgerald, F.D., Hume, S.A., McGough, G., Damen, K., 2014. Ferrybridge CCPilot100+ operating experience and final test results. Energy Procedia 63, 6239–6251. http://dx.doi.org/10.1016/j.egypro.2014.11.655.

Flude, S., Johnson, G., Gilfillan, S.M.V., Haszeldine, R.S., 2016. Inherent tracers for carbon capture and storage in sedimentary formations: composition and applications. Environ. Sci. Technol. 50, 7939–7955. http://dx.doi.org/10.1021/acs.est.6b01548.

Freifeld, B.M., 2005. The U-tube: a novel system for acquiring borehole fluid samples from a deep geologic CO_2 sequestration experiment. J. Geophys. Res. 110. http://dx.doi.org/10.1029/2005JB003735.

Freundt, F., Schneider, T., Aeschbach-Hertig, W., 2013. Response of noble gas partial pressures in soil air to oxygen depletion. Chem. Geol. 339, 283–290. http://dx.doi.org/10.1016/j.chemgeo.2012.07.026.

Güleç, N., Hilton, D.R., 2016. Turkish geothermal fields as natural analogues of CO_2 storage sites: gas geochemistry and implications for CO_2 trapping mechanisms.

Geothermics 64, 96–110. http://dx.doi.org/10.1016/j.geothermics.2016.04.008.
Garcia, B., Billiot, J.H., Rouchon, V., Mouronval, G., Lescanne, M., Lachet, V., Aimard, N., 2012. A geochemical approach for monitoring a CO_2 pilot site: rousse, France. a major gases, CO_2 –Carbon isotopes and noble gases combined approach. Oil Gas Sci. Technol. – Revue d'IFP Energies nouvelles 67, 341–353. http://dx.doi.org/10.2516/ogst/2011154.
Gilfillan, S.M.V., Haszeldine, R.S., 2011. Report on noble gas, carbon stable isotope and HCO_3 measurements from the Kerr Quarter and surrounding area, Goodwater, Saskatchewan. In: Sherk, G.W. (Ed.), The Kerr Investigation – Final Report, pp. 77–102.
Gilfillan, S.M.V., Lollar, B.S., Holland, G., Blagburn, D., Stevens, S., Schoell, M., Cassidy, M., Ding, Z., Zhou, Z., Lacrampe-Couloume, G., Ballentine, C.J., 2009. Solubility trapping in formation water as dominant CO_2 sink in natural gas fields. Nature 458, 614–618. http://dx.doi.org/10.1038/nature07852.
Gilfillan, S.M.V., Wilkinson, M., Haszeldine, R.S., Shipton, Z.K., Nelson, S.T., Poreda, R.J., 2011. He and Ne as tracers of natural CO_2 migration up a fault from a deep reservoir. Int. J. Greenh. Gas Control 5, 1507–1516. http://dx.doi.org/10.1016/j.ijggc.2011.08.008.
Gilfillan, S., Haszedline, S., Stuart, F., Gyore, D., Kilgallon, R., Wilkinson, M., 2014. The application of noble gases and carbon stable isotopes in tracing the fate, migration and storage of CO_2. Energy Procedia 63, 4123–4133. http://dx.doi.org/10.1016/j.egypro.2014.11.443.
Gilfillan, S.M.V., Sherk, G.W., Poreda, R.J., Haszeldine, R.S., 2017. Using noble gas fingerprints at the Kerr Farm to assess CO_2 leakage allegations linked to the Weyburn-Midale CO_2 monitoring and storage project. Int. J. Greenh. Gas Control 63, 215–225. http://dx.doi.org/10.1016/j.ijggc.2017.05.015.
Greene, S., Battye, N., Clark, I., Kotzer, T., Bottomley, D., 2008. Canadian Shield brine from the Con Mine, Yellowknife, NT, Canada: noble gas evidence for an evaporated Palaeozoic seawater origin mixed with glacial meltwater and Holocene recharge. Geochim. Cosmochim. Acta 72, 4008–4019. http://dx.doi.org/10.1016/j.gca.2008.05.058.
Györe, D., Stuart, F.M., Gilfillan, S.M.V., Waldron, S., 2015. Tracing injected CO_2 in the Cranfield enhanced oil recovery field (MS, USA) using He, Ne and Ar isotopes. Int. J. Greenh. Gas Control 42, 554–561. http://dx.doi.org/10.1016/j.ijggc.2015.09.009.
Györe, D., Gilfillan, S.M.V., Stuart, F.M., 2017. Tracking the interaction between injected CO_2 and reservoir fluids using noble gas isotopes in an analogue of large-scale carbon capture and storage. Appl. Geochem. 78, 116–128. http://dx.doi.org/10.1016/j.apgeochem.2016.12.012.
Haese, R.R., Black, J.R., Vu, H.P., 2016. The impact of CO_2 impurities (SO_2, NOx, O_2) on fluid-rock reactions and water quality in a CO_2 storage reservoir (CO_2CRC Report No. RPT16-5501).
Holland, G., Gilfillan, S., 2013. Application of noble gases to the viability of CO_2 storage. In: Burnard, P. (Ed.), The Noble Gases as Geochemical Tracers. Springer Berlin Heidelberg, Berlin Heidelberg, pp. 177–223.
IPCC, 2013. Climate Change 2013: The Physical Science Basis: Working Group I Contribution to the Fifth Assessment Report of the Intergovernmental Panel on Climate Change. Cambridge University Press, Cambridge, UK.
International Energy Agency, 2014. Energy Technology Perspectives 2014 (Executive Summary). International Energy Agency, Paris.
Jensen, G.K.S., Rostron, B.J., 2014. Monitoring and verification of injected CO_2 at the Aquistore site, Saskatchewan, Canada: sampling of Tertiary, Cretaceous, and Devonian aquifers to establish a baseline and continued monitoring during CO_2 injection. Energy Procedia 63, 4145–4149. http://dx.doi.org/10.1016/j.egypro.2014.11.445.
Johnson, G., Mayer, B., Nightingale, M., Shevalier, M., Hutcheon, I., 2011a. Using oxygen isotope ratios to quantitatively assess trapping mechanisms during CO_2 injection into geological reservoirs: the Pembina case study. Chem. Geol. 283, 185–193. http://dx.doi.org/10.1016/j.chemgeo.2011.01.016.
Johnson, G., Mayer, B., Shevalier, M., Nightingale, M., Hutcheon, I., 2011b. Tracing the movement of CO_2 injected into a mature oilfield using carbon isotope abundance ratios: the example of the Pembina Cardium CO_2 Monitoring project. Int. J. Greenh. Gas Control 5, 933–941. http://dx.doi.org/10.1016/j.ijggc.2011.02.003.
Kharaka, Y.K., Cole, D.R., Thordsen, J.J., Kakouros, E., Nance, H.S., 2006. Gas-water-rock interactions in sedimentary basins: CO_2 sequestration in the Frio Formation, Texas, USA. J. Geochem Explor. 89, 183–186. http://dx.doi.org/10.1016/j.gexplo.2005.11.077.
Kharaka, Y.K., Thordsen, J.J., Hovorka, S.D., Seay Nance, H., Cole, D.R., Phelps, T.J., Knauss, K.G., 2009. Potential environmental issues of CO_2 storage in deep saline aquifers: geochemical results from the Frio-I Brine Pilot test, Texas, USA. Appl. Geochem. 24, 1106–1112. http://dx.doi.org/10.1016/j.apgeochem.2009.02.010.
Kipfer, R., Aeschbach-Hertig, W., Peeters, F., Stute, M., 2002. Noble gases in lakes and ground waters. Rev. Mineral. Geochem. 47, 615–700. http://dx.doi.org/10.2138/rmg.2002.47.14.
Kroopnick, P., Craig, H., 1972. Atmospheric oxygen: isotopic composition and solubility fractionation. Science 175, 54–55. http://dx.doi.org/10.1126/science.175.4017.54.
Lee, J.-Y., Marti, K., Severinghaus, J.P., Kawamura, K., Yoo, H.-S., Lee, J.B., Kim, J.S., 2006. A redetermination of the isotopic abundances of atmospheric Ar. Geochim. Cosmochim. Acta 70, 4507–4512. http://dx.doi.org/10.1016/j.gca.2006.06.1563.
Lee, A.S., Eslick, J.C., Miller, D.C., Kitchin, J.R., 2013. Comparisons of amine solvents for post-combustion CO_2 capture: a multi-objective analysis approach. Int. J. Greenh. Gas Control 18, 68–74. http://dx.doi.org/10.1016/j.ijggc.2013.06.020.
Lu, J., Kharaka, Y.K., Thordsen, J.J., Horita, J., Karamalidis, A., Griffith, C., Hakala, J.A., Ambats, G., Cole, D.R., Phelps, T.J., Manning, M.A., Cook, P.J., Hovorka, S.D., 2012. CO_2-rock-brine interactions in Lower Tuscaloosa Formation at Cranfield CO_2 sequestration site, Mississippi, U.S.A. Chem. Geol. 291, 269–277. http://dx.doi.org/10.1016/j.chemgeo.2011.10.020.
Mackintosh, S.J., Ballentine, C.J., 2012. Using $^3He/^4He$ isotope ratios to identify the source of deep reservoir contributions to shallow fluids and soil gas. Chem. Geol. 304-305, 142–150. http://dx.doi.org/10.1016/j.chemgeo.2012.02.006.
Mamyrin, B.A., Anufrijev, G.S., Kamenskii, I.L., Tolstikhin, I.N., 1970. Determination of the isotopic composition of atmospheric helium. Geochem. Int. 7, 498–505.
Martens, S., Kempka, T., Liebscher, A., Lüth, S., Möller, F., Myrttinen, A., Norden, B., Schmidt-Hattenberger, C., Zimmer, M., Kühn, M., 2012. Europe's longest-operating on-shore CO_2 storage site at Ketzin, Germany: a progress report after three years of injection. Environ. Earth Sci. 67, 323–334. http://dx.doi.org/10.1007/s12665-012-1672-5.
Mayer, B., Shevalier, M., Nightingale, M., Kwon, J.-S., Johnson, G., Raistrick, M., Hutcheon, I., Perkins, E., 2013. Tracing the movement and the fate of injected CO2 at the IEA GHG Weyburn-Midale CO_2 Monitoring and Storage project (Saskatchewan, Canada) using carbon isotope ratios. Int. J. Greenh. Gas Control 16, S177–S184. http://dx.doi.org/10.1016/j.ijggc.2013.01.035.
Mayer, B., Humez, P., Becker, V., Dalkhaa, C., Rock, L., Myrttinen, A., Barth, J.A.C., 2015. Assessing the usefulness of the isotopic composition of CO2 for leakage monitoring at CO2 storage sites: a review. Int. J. Greenh. Gas Control 37, 46–60. http://dx.doi.org/10.1016/j.ijggc.2015.02.021.
McDougall, I., Harrison, T.M., 1999. Geochronology and Thermochronology by the $^{40}Ar/^{39}Ar$ Method, 2nd edition. Oxford University Press.
Moser, P., Schmidt, S., Stahl, K., Vorberg, G., Lozano, G.A., Stoffregen, T., Rösler, F., 2014. Demonstrating emission reduction – Results from the post-combustion capture pilot plant at Niederaussem. Energy Procedia 63, 902–910. http://dx.doi.org/10.1016/j.egypro.2014.11.100.
Myrttinen, A., Becker, V., van Geldern, R., Würdemann, H., Morozova, D., Zimmer, M., Taubald, H., Blum, P., Barth, J.A.C., 2010. Carbon and oxygen isotope indications for CO_2 behaviour after injection: first results from the Ketzin site (Germany). Int. J. Greenh. Gas Control 4, 1000–1006. http://dx.doi.org/10.1016/j.ijggc.2010.02.005.
Nelson, S.T., 2000. A simple, practical methodology for routine VSMOW/SLAP normalization of water samples analyzed by continuous flow methods. Rapid Commun. Mass Spectrom. 14, 1044–1046. http://dx.doi.org/10.1002/1097-0231(20000630)14:12<1044:AID-RCM987>3.0.CO;2-3.
Newell, D.L., Larson, T.E., Perkins, G., Pugh, J.D., Stewart, B.W., Capo, R.C., Trautz, R.C., 2014. Tracing CO_2 leakage into groundwater using carbon and strontium isotopes during a controlled CO_2 release field test. Int. J. Greenh. Gas Control 29, 200–208. http://dx.doi.org/10.1016/j.ijggc.2014.08.015.
Nisi, B., Vaselli, O., Tassi, F., de Elio, J., Huertas, A.D., Mazadiego, L.F., Ortega, M.F., 2013. Hydrogeochemistry of surface and spring waters in the surroundings of the CO_2 injection site at Hontomín–Huermeces (Burgos, Spain). Int. J. Greenh. Gas Control 14, 151–168. http://dx.doi.org/10.1016/j.ijggc.2013.01.012.
Nowak, M.E., van Geldern, R., Myrttinen, A., Zimmer, M., Barth, J.A.C., 2014. High-resolution stable carbon isotope monitoring indicates variable flow dynamic patterns in a deep saline aquifer at the Ketzin pilot site (Germany). Appl. Geochem. 47, 44–51. http://dx.doi.org/10.1016/j.apgeochem.2014.05.009.
Ozima, M., Podosek, F.A., 2002. Noble Gas Geochemistry, 2nd edition. Cambridge University Press.
PACT. 2016. PACT Website [WWW Document]. URL http://www.pact.ac.uk/facilities/PACT-Core-Facilities/ (Accessed 23 January 2017).
Paterson, L., Boreham, C., Bunch, M., Ennis-King, J., Freifeild, B.M., Haese, R., Jenkins, C., Raab, M., Singh, R., Stalker, L., 2011. The CO2CRC Otway stage 2B residual saturation and dissolution test: test concept, implementation and data collected (CO2CRC Report No. RPT11-3158).
Paterson, L., Boreham, C., Bunch, M., Dance, T., Ennis-King, J., Freifeld, B., Haese, R., Jenkins, C., LaForce, T., Raab, M., Singh, R., Stalker, L., Zhang, Y., 2013. Overview of the CO_2CRC Otway Residual Saturation and Dissolution Test. Energy Procedia 37, 6140–6148. http://dx.doi.org/10.1016/j.egypro.2013.06.543.
Podosek, F.A., Bernatowicz, T.J., Kramer, F.E., 1981. Adsorption of xenon and krypton on shales. Geochim. Cosmochim. Acta 45, 2401–2415. http://dx.doi.org/10.1016/0016-7037(81)90094-6.
Raistrick, M., Mayer, B., Shevalier, M., Perez, R.J., Hutcheon, I., Perkins, E., Gunter, B., 2006. Using chemical and isotopic data to quantify ionic trapping of injected carbon dioxide in oil field brines. Environ. Sci. Technol. 40, 6744–6749. http://dx.doi.org/10.1021/es060551a.
Rostron, B., White, D., Hawkes, C., Chalaturnyk, R., 2014. Characterization of the Aquistore CO_2 project storage site, Saskatchewan, Canada. Energy Procedia 63, 2977–2984. http://dx.doi.org/10.1016/j.egypro.2014.11.320.
Scott, V., Gilfillan, S., Markusson, N., Chalmers, H., Haszeldine, R.S., 2012. Last chance for carbon capture and storage. Nat. Clim. Change 3, 105–111. http://dx.doi.org/10.1038/nclimate1695.
Serno, S., Johnson, G., LaForce, T.C., Ennis-King, J., Haese, R.R., Boreham, C.J., Paterson, L., Freifeld, B.M., Cook, P.J., Kirste, D., Haszeldine, R.S., Gilfillan, S.M.V., 2016. Using oxygen isotopes to quantitatively assess residual CO_2 saturation during the CO2CRC Otway Stage 2B Extension residual saturation test. Int. J. Greenh. Gas Control 52, 73–83. http://dx.doi.org/10.1016/j.ijggc.2016.06.019.
Serno, S., Flude, S., Johnson, G., Mayer, B., Karolytė, R., Haszeldine, R.S., Gilfillan, S., 2017. Oxygen isotopes as a tool to quantify reservoir-scale CO_2 pore-space saturation. Int. J. Greenh. Gas Control 63, 370–385. http://dx.doi.org/10.1016/j.ijggc.2017.06.009.
Shelton, J.L., McIntosh, J.C., Hunt, A.G., Beebe, T.L., Parker, A.D., Warwick, P.D., Drake, R.M., McCray, J.E., 2016. Determining CO_2 storage potential during miscible CO_2 enhanced oil recovery: noble gas and stable isotope tracers. Int. J. Greenh. Gas Control 51, 239–253. http://dx.doi.org/10.1016/j.ijggc.2016.05.008.
Shevalier, M., Nightingale, M., Johnson, G., Mayer, B., Perkins, E., Hutcheon, I., 2009. Monitoring the reservoir geochemistry of the Pembina Cardium CO_2 monitoring project, Drayton Valley, Alberta. Energy Procedia 1, 2095–2102. http://dx.doi.org/

10.1016/j.egypro.2009.01.273.
Shevalier, M., Nightingale, M., Mayer, B., Hutcheon, I., Durocher, K., Perkins, E., 2013. Brine geochemistry changes induced by CO_2 injection observed over a 10 year period in the Weyburn oil field. Int. J. Greenh. Gas Control 16, S160–S176. http://dx.doi.org/10.1016/j.ijggc.2013.02.017.
Stéphenne, K., 2014. Start-up of world's first commercial post-combustion coal fired CCS project: contribution of shell cansolv to SaskPower boundary dam ICCS project. Energy Procedia 63, 6106–6110. http://dx.doi.org/10.1016/j.egypro.2014.11.642.
Torgersen, T., Kennedy, B.M., 1999. Air-Xe enrichments in Elk Hills oil field gases: role of water in migration and storage. Earth Planet. Sci. Lett. 167, 239–253. http://dx.doi.org/10.1016/S0012-821X(99)00021-7.
Uchida, T., Goto, T., Yamada, T., Kiga, T., Spero, C., 2013. Oxyfuel combustion as CO_2 capture technology advancing for practical use − Callide oxyfuel project. Energy Procedia 37, 1471–1479. http://dx.doi.org/10.1016/j.egypro.2013.06.022.
Usdowski, E., Hoefs, J., 1988. $^{13}C/^{12}C$ fractionation during the chemical absorption of CO_2 gas by the NH_3—NH_4Cl buffer. Chemical Geol.: Isotope Geosci. Sect. 73, 79–85. http://dx.doi.org/10.1016/0168-9622(88)90022-X.
Warr, O., Rochelle, C.A., Masters, A., Ballentine, C.J., 2015. Determining noble gas partitioning within a CO_2-H_2O system at elevated temperatures and pressures. Geochim. Cosmochim. Acta 159, 112–125. http://dx.doi.org/10.1016/j.gca.2015.03.003.
Watson, M.N., Boreham, C.J., Tingate, P.R., 2004. Carbon dioxide and carbonate cements in the Otway Basin: implications for geological storage of carbon dioxide. APPEA J. 44, 703–720.
Whittaker, S., Worth, K., 2011. Aquistore: a fully integrated demonstration of the capture, transportation and geologic storage of CO_2. Energy Procedia 4, 5607–5614. http://dx.doi.org/10.1016/j.egypro.2011.02.550.
Widory, D., 2006. Combustibles, fuels and their combustion products: a view through carbon isotopes. Combust. Theor. Model. 10, 831–841. http://dx.doi.org/10.1080/13647830600720264.
Worth, K., White, D., Chalaturnyk, R., Sorensen, J., Hawkes, C., Rostron, B., Johnson, J., Young, A., 2014. Aquistore project measurement, monitoring, and verification: from concept to CO_2 injection. Energy Procedia 63, 3202–3208. http://dx.doi.org/10.1016/j.egypro.2014.11.345.